Chapter 5:   Tailings Solids and Porewaters

5.1   Processes Affecting the Geochemical Evolution and Diagenesis of the Tailings

Tailings typically comprise complex mixtures of various lithogenic (primary minerals and weathering products), process (chemicals and spent reagents), biogenic (products of biological activity, such as sewage) and authigenic (components that form after deposition) phases. As time progresses and the tailings sediments accumulate, the chemical make-up of the solids and porewaters change due to various post-depositional reactions.

The term "sediment diagenesis" is used to describe the post depositional transformations that occur within the sediment column over time. Several factors influence trace metal and radionuclide diagenesis of which three of the most important are (Berner, 1980):

- The nature and content of organic matter in sediments;

- Sediment and water-column redox potential; and

- The specific reactivity of mineral phases and porewater solutes.

Although each of these factors represents a unique influence on trace metal and radionuclide diagenesis, their respective effects are difficult to isolate because of the interdependent biogeochemical relationships associated with the tailings sedimentary system.

A knowledge of the diagenetic state is therefore critical to understanding the processes governing the behaviour and mobility of tailings constituents, and accordingly, assessing the reactivity of potentially toxic components. In the following sections, the principles of sediment diagenesis are used to assess the geochemical evolution of the Ranger tailings.

5.1.1   Geochemical Processes

Tailings are, in essence, a geochemical system that is in chemical disequilibrium with the surrounding environment. With time, therefore, the geochemical system will continue to change as the various components, aqueous and solid species, react to attain equilibrium conditions.

The extent and rate at which the tailings achieve equilibrium depends on the initial tailings mineralogy and geochemistry (Hutchison and Ellison, 1992). In this context, Chapter 5 examines the mineralogy, geochemistry, solid state speciation and porewater chemistry of the tailings pile to define the key hydrogeochemical and microbially mediated processes that govern the solubility and partitioning of radionuclides. Acquisition of such knowledge is critical in the development of a geochemical model (Chapter 7) to predict radionuclide speciation and the evolution and long term geochemical stability of the tailings pile.

In a typical sulfuric acid-leach/tailings neutralisation uranium mill (see Figure 1.1), the geochemical reactions resulting from the interaction of the acid-lixiviant and the uraniferous ore are as described by Markos (1979). First, ferric ion (Fe^{3+}) is required in the leach solution to achieve rapid and complete oxidation of tetravalent uranium. Uraninite ($UO_2(s)$) is the principal uranium mineral:

$$UO_2(s) + 2Fe^{3+} \leftrightarrow UO_2^{2+} + 2Fe^{2+} \dots\dots\dots(5.1)$$
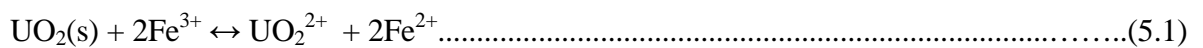
The addition of sufficient oxidant, such as pyrolusite (MnO_2) or sodium chlorate ($NaClO_3$) ensures that iron is present predominantly as Fe^{3+}:

$$2Fe^{2+} + MnO_2 + 4H^+ \leftrightarrow 2Fe^{3+} + Mn^{2+} + 2H_2O\dots\dots\dots(5.2)$$

The second part of the leaching oxidation process is the addition of dilute sulfuric acid to control the pH at around 1.8. At this pH the sulfuric acid ionizes to sulfate, bisulfate and hydrogen ion. For example, the sulfate ion complexes uranyl as follows:

$$UO_2^{2+} + H_2SO_4 \leftrightarrow UO_2SO_4 + 2H^+ \dots (5.3)$$
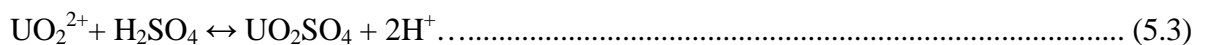
Acid is not consumed directly by dissolution of UO_2 but is required to oxidize ferrous ion to ferric ion - reaction (5.2). In addition to uranium, the oxidation process also causes the dissolution of gangue minerals (carbonates and aluminosilicates) and accessory metal/metalloid sulfides. For example:
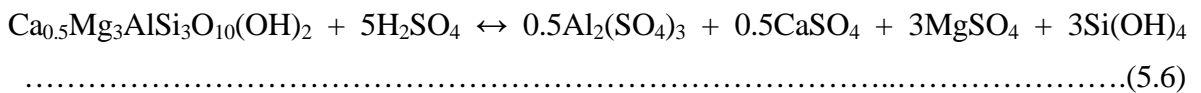
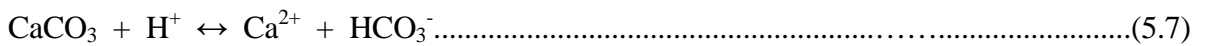- Dolomite/Magnesite (Gangue Mineral)

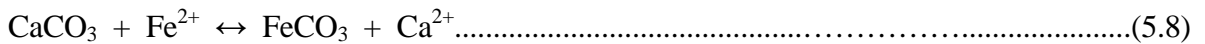$$(Ca, Mg)(CO_3)_2 + 2H_2SO_4 \leftrightarrow CaSO_4 + MgSO_4 + 2H_2O + 2CO_2\dots\dots(5.4)$$

- Covellite (Metal Sulfide)

$$CuS + H_2SO_4 \leftrightarrow H_2S + Cu^{2+} + SO_4^{2-} \dots\dots(5.5)$$

- Aluminosilicates (Gangue minerals)

$$Ca_{0.5}Mg_3AlSi_3O_{10}(OH)_2 + 5H_2SO_4 \leftrightarrow 0.5Al_2(SO_4)_3 + 0.5CaSO_4 + 3MgSO_4 + 3Si(OH)_4$$
………………………………………………………………………..………………….(5.6)

- Calcite dissolution (congruent)

$$CaCO_3 + H^+ \leftrightarrow Ca^{2+} + HCO_3^- ....……........................(5.7)$$

- Calcite dissolution (incongruent)

$$CaCO_3 + Fe^{2+} \leftrightarrow FeCO_3 + Ca^{2+}...............................……………......................(5.8)$$

- Siderite dissolution

$$FeCO_3 + H^+ \leftrightarrow Fe^{2+} + HCO_3^-…...............................………...(5.9)$$
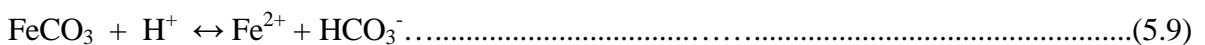
Because acidic (pH 2) uranium tailings water is high in aqueous sulfate and near gypsum saturation, the addition of slaked lime ($Ca(OH)_2(l)$) to neutralise the tailings to pH 7 to 8 initiates gypsum precipitation:

$$Ca^{2+} + SO_4^{2-} + 2H_2O \leftrightarrow CaSO_4.2H_2O…...……...............(5.10)$$
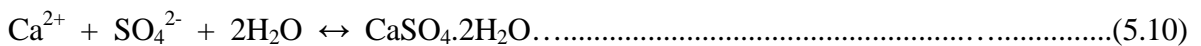
The addition of lime also initiates the precipitation of a number of other secondary minerals as described by Morin (1983): ferrihydrite ($Fe(OH)_3$), gibbsite ($Al(OH)_3$), alumino-silicates ($Al_2Si_2O_5(OH)_4$) and amorphous silica ($SiO_2(am)$). The formation of these secondary minerals creates a highly reactive geochemical environment that affects the solubility of radionuclides and metals via direct precipitation - dissolution, co-precipitation and sorption processes.

The tailings also contain significant quantities of microbiologically reactive organic and nitrogen compounds:

- Shellsol (high flash point kerosene – the major hydrocarbon used in the solvent extraction of the uraniferous ore);

- Residual iso-tridecanol and trialkylamines degradation products from the solvent extraction process;

- Flocculants to enhance thickener performance – cationic polyacrylamides; and

- Sewage effluent: Note this is not a by-product of the milling process but a separate waste stream that is co-disposed with the tailings. Sewage effluent is a biologically reactive medium and as such is a principal fuel for micro-organisms.

The presence of organic matter in the tailings is significant as several studies (Sholkovitz, 1973; Froelich et al. 1979; Van der Weijden, 1992; Postma and Jakobsen, 1996) on natural sediments show that post-depositional reactions are primarily fuelled by the microbially-mediated decomposition of organic matter. These mechanisms and their profound effect on tailings authigenesis are discussed in the following sections and Chapter 6.

5.1.2   Diagenetic Processes

Organic matter is the key to any biogeochemical consideration of sediment diagenesis, not only because it represents chemical potential energy capable of driving diagenetic reactions but also because it plays a critical role in cycling radionuclides and trace metals. This metal cycling occurs as a result of the redox couple that forms between the electron donor (organic matter) and an in-situ oxidant that accepts electrons from organic matter (Stumm and Morgan, 1996).

While the transfer of electrons between organic substrate and oxidant occurs spontaneously, heterotrophic bacteria are known to catalyze the transfer, considerably increasing the rate of organic matter oxidation. A schematic representing this process is shown in Figure 5.1.
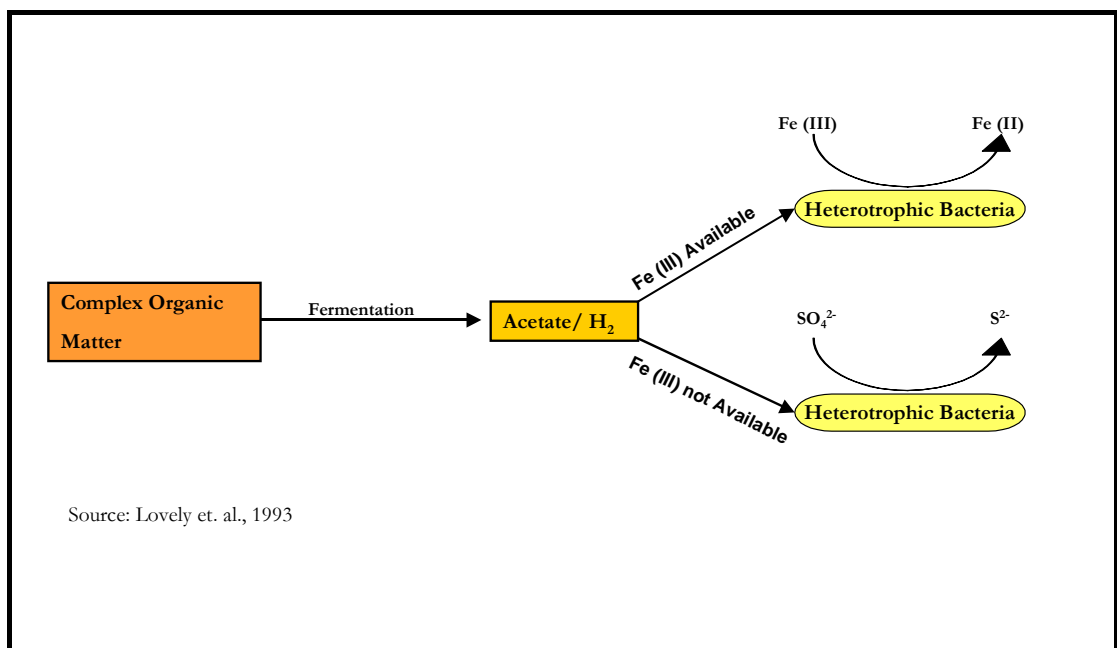

Figure 5.1:   Schematic of microbially mediated redox processes

During this enzymatic process the bacteria take advantage of chemical potential energy found in the organic matter and use the energy released in the electron transfer reactions to drive their own metabolism (Stumm and Morgan, 1996). Kimber and Moen (1992) confirmed the

presence of heterotrophic bacteria in the Ranger tailings and hence the potential for microbially mediated organic matter oxidation. On this basis, organic matter diagenesis was evaluated as a possible mechanism to explain the observed mineralogical and porewater trends in the tailings pile. Evidence in support of this tenet is provided in the following sections and Chapter 6.

The oxidation of organic matter proceeds via the reduction of various oxidants in their decreasing free energy yield per mole of organic carbon oxidised. Reactions releasing the highest free energy yield ($-\Delta G_r^{\circ}$) also produce the greatest available energy for bacterial utilisation.

As summarised in Table 5.1, the order of oxidation proceeds with the initial removal of dissolved oxygen followed by the reduction of nitrate, manganese(IV), uranium(VI), iron(III), molybdenum(VI) and sulfate. These reactions best represent the key redox couples within the tailings pile and are well documented as being mediated by heterotrophic bacteria (Cochran et al. 1986; Lovely et al. 1993; Ribet et al. 1995; Stumm and Morgan, 1996; Abdelouas et al. 1999).

As each of the equations in Table 5.1 represents an equilibrium redox state it is more appropriate and numerically convenient to use the parameter pε or electron activity. This is the negative logarithm of an assumed activity of electrons in solution, just as pH is the negative logarithm of the activity of protons in solution (Krauskopf and Bird, 1995). In this context, pε measures the ability of an environment such as the tailings pile to supply electrons to an oxidising agent, such as those described in Table 5.1, from a reducing agent such as organic matter.

As organic matter is a source of electrons and the oxidants a sink, the redox potential is governed by the flow of electrons between these two pools. In the tailings pile, the redox state of any given horizon is the result of a balance between the content and lability of organic matter in the tailings in concert with the quantity and type of available oxidant (Froelich et al. 1979).

Table 5.1: Half cell reactions of oxidants present in the tailings pile and their associated free energies and electron activities.

[*]Half Cell Reactions	ΔG_r kJ mol^{-1}	pε
Oxidation Reaction		
$CH_2O + H_2O \leftrightarrow HCO_3^- + 5H^+ + 4e^-$		
Reduction Reactions		
$O_2 + 4H^+ + 4e^- \leftrightarrow 2H_2O$	-474	13.76
$0.8NO_3^- + 4.8H^+ + 4e^- \leftrightarrow 0.4N_2 + 2.4H_2O$	-480	12.00
$2MnO_2 + 2HCO_3^- + 6H^+ + 4e^- \leftrightarrow 2MnCO_3 + 4H_2O$	-478	8.60
$4Fe(OH)_3 + 4HCO_3^- + 8H^+ + 4e^- \leftrightarrow 4FeCO_3 + 12H_2O$	-376	0.70
$2UO_2(SO_4)_2^{2-} + 4e^- \leftrightarrow 2UO_2(am) + 4SO_4^{2-}$	-56	0.17
$2UO_2(CO_3)_2^{2-} + 4H^+ + 4e^- \leftrightarrow 2UO_2(am) + 4HCO_3^-$	-146	0.11
$2MoO_4^{2-} + 8H^+ + 4e^- \leftrightarrow 2MoO_2 + 4H_2O$	-342	-1.86
$0.5SO_4^{2-} + 4.5H^+ + 4e^- \leftrightarrow 0.5HS^- + 2H_2O$	-96	-3.76

[*] Equations are representative of the following average porewater concentrations and conditions: $[U] = 1.7 \times 10^{-6}$ mol L^{-1}; $[NO_3^-] = 1.1 \times 10^{-3}$ mol L^{-1}; $[SO_4^{2-}] = 0.25$ mol L^{-1}; pH = 7; $[Mo] = 2.0 \times 10^{-6}$ mol L^{-1}; $[HCO_3^-] = 2.5 \times 10^{-4}$ mol L^{-1}; 25°C; 1 bar. ΔG_r and pε were calculated from thermodynamic data reported by Stumm and Morgan (1996) and Grenthe et al. (1992). CH_2O is used to represent organic matter.

Since the pε is the electron activity at equilibrium and therefore a measure of the relative tendency of a solution to accept or transfer electrons (Stumm and Morgan 1996), it can be related to the free energy change of reaction (ΔG) via the Nernst equation:

$$p\varepsilon = -\Delta G/(2.303RT) \ldots\ldots\ldots\ldots\ldots\ldots\ldots\ldots\ldots\ldots\ldots\ldots\ldots\ldots\ldots\ldots\ldots\ldots\ldots(5.11)$$

where R is the universal gas constant and T is temperature expressed in Kelvin.

On this basis, the succession of microbially mediated reactions as described in Table 5.1 are in order of decreasing redox potential (pε). That is, the organic matter reductant (CH_2O) will transfer electrons to the lowest unoccupied energy level (O_2) and as more electrons become available, successive levels e.g. NO_3^-, MnO_2, $UO_2(SO_4)_2^{2-}$ and so on will be filled (Stumm and Morgan, 1996). The result is both a temporal or spatial sequence of bacterial species beginning with aerobic bacteria followed by nitrate reducers, and so on, finally ending with fermentors, sulfate reducers and methanogens. There is little overlap between these groups as the oxidants

or metabolites of one group are usually toxic to another (Froelich et al. 1979), hence the various bacterial assemblages closely follow the redox state of the sediment column as shown in Figure 5.2.
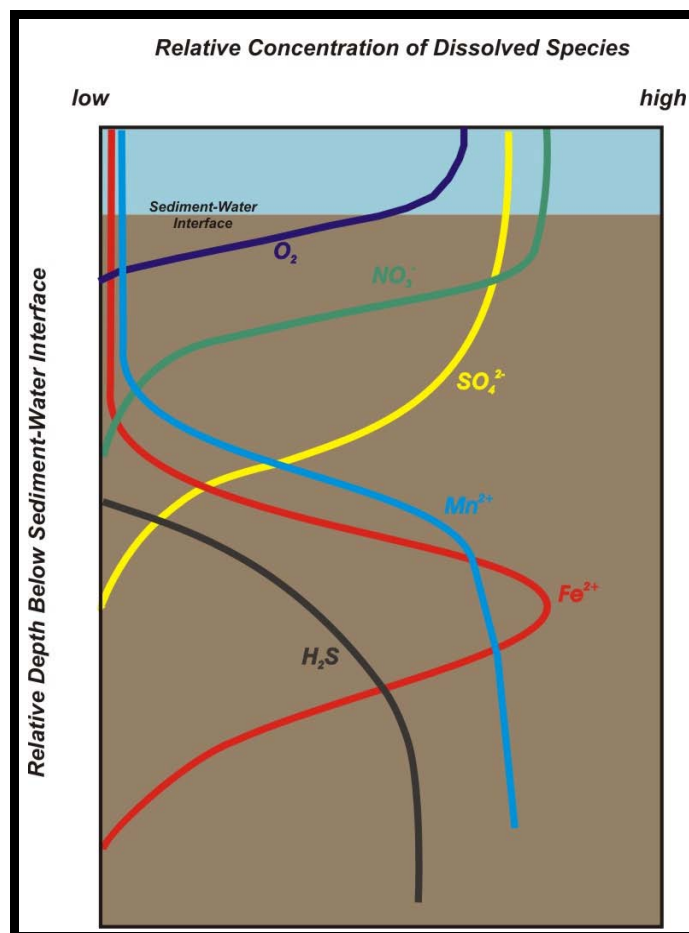

Figure 5.2:   Theoretical redox zonation and dissolved species distribution of submerged sediments

As organic matter diagenesis proceeds, reaction by-products such as HCO_3^-, HS^- and metals (Fe, Mn, Co, Ni , Pb, Cd) mobilised by the reductive dissolution of Fe/Mn oxyhydroxides react to form authigenic carbonate and sulfide minerals. The formation of authigenic uraninite is known to occur within the tailings pile and is of particular interest as this phase may control the solubility of U in porewaters. The amorphous form of uraninite was selected as being the most likely phase to form under the prevailing geochemical environment of the tailings pile. In this context, the thermodynamic calculations shown in Table 5.1, indicate that amorphous uraninite may precipitate ($p\varepsilon$ 0.11-0.17) at a similar redox potential to that required for the reductive dissolution of ferrihydrite ($p\varepsilon$ 0.7). The sequential occurrence of these processes may in part be explained by dissimilatory Fe(III) reducing bacteria that can obtain energy growth by reducing

U(VI) to insoluble U(IV) (Lovely et al. 1991). These phases and their role in the geochemical evolution of the tailings pile are discussed in the following sections and Chapter 6.

The release of secondary metabolites by bacteria, in conjunction with vertical zonation of bacterial assemblages, allows the use of dissolved metabolite profiles as indicators of redox conditions in sediments. For this study, the metabolites, O_2, NO_3^-, Mn, U, Fe and Mo were measured to infer the redox state of the tailings profile. Direct Eh measurements of the tailings-porewater system via a platinum electrode were also recorded but these data only provide a qualitative and macro insight into the prevailing redox conditions of the tailings pile. This is because some of the reactions (such as those involving oxygen) that determine redox potentials are slow, so that instantaneous readings with a platinum electrode do not give valid equilibrium potential differences (Krauskopf and Bird, 1995).

As a result of these varying reaction rates, it is possible to have several different redox states within the same microenvironment or locale within the tailings pile. Therefore, developing a quantitative exposition of the redox conditions and processes within the tailings pile will largely depend on understanding the dynamics of the tailings pore-water system via the aforementioned bacterial metabolites rather than relying on qualitative macro Eh measurements.

5.1.3   Effect of Redox Potential on Uranium and Trace Metal Distribution within the Tailings Pile

There are two ways in which redox potential can effect metal partitioning within the tailings pile:

- Alteration of the oxidation state of certain metals such Fe, Mn, U and Mo; and

- Alteration of the oxidation state of ligand atoms (i.e. N and S) within a complexing substrate.

Iron and manganese are unique in that they are both abundant in the tailings pile and in their oxidised forms, exist as solids with strong sorption characteristics (Tessier et al. 1996). Thus, even though other metals may not be subject to direct changes in oxidation state, they can be indirectly affected by redox potential as a result of being scavenged by or co-precipitated with Fe and Mn oxides. The result is often the formation of a metal-enriched, oxide bearing sediment layer near the sediment – water interface (Tessier et al. 1996). At the base of such a

layer, where the redox potential is lower, Fe and Mn oxides undergo reductive dissolution and are remobilized to the interstitial waters. Some of the reduced ionic iron and manganese diffuse upwards, encounter oxygen and reprecipitate as amorphous oxides with concomitant co precipitation of other metals. Thus, porewater profiles of Fe and Mn typically show strong metal concentration gradients spatially coincident with the base of an enriched, solid phase layer (Pedersen et al. 1986).

Redox potential can also affect the metal partitioning within the tailings pile by altering the oxidation state of certain ligands such as sulfur and nitrogen. In oxic porewaters, sulfur primarily exists as sulfate which is a weak complexer of metals (Stumm and Morgan, 1996). However in anoxic porewaters, sulfur (as HS^-) is a highly reactive ligand that not only complexes with most metals, but also forms insoluble metal-sulfide precipitates (Ritcey, 1989). Similarly, in oxic porewaters, nitrogen exists primarily as NO_3^- but is progressively reduced to nitrite (NO_2^-) then ammonium (NH_4^+) as the redox potential decreases to form anoxic conditions. Ammonium is a monovalent cation that can alter the partitioning of other metals within the tailings by cation exchange mechanisms such as the substitution of readily exchangeable ions on the surface of clay minerals such as K-feldspar:

$$KAlSi_3O_8(s) + NH_4^+(aq) \leftrightarrow NH_4AlSi_3O_8(s) + K^+(aq) \dots\dots\dots\dots\dots\dots\dots\dots\dots.(5.12)$$
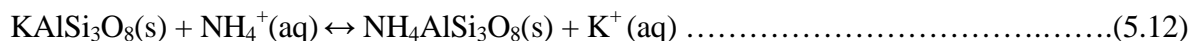
5.1.4   Authigenic Phases

In tailings where organic matter oxidises relatively quickly, it is possible for metabolite concentrations within the interstitial waters to increase and exceed the solubility products of their respective solid phases. This often results in the formation of secondary or authigenic minerals, which can govern the partitioning and mobility of radionuclides and trace metals within the tailings pile. The most common authigenic phases, and those particularly relevant to this study, include carbonates, oxides of Fe and Mn and sulfides (Calvert, 1976; Luther and Tsamakis, 1989).

5.1.4.1 Carbonates

Trace metals and radium are known to adsorb and coprecipitate with carbonates (Framson and Leckie, 1978; Lorens, 1981; Landa, 1986; Mucci, 1988; Ritcey, 1989). Chemogenic precipitation of calcite and aragonite is thought to occur in anoxic environments where the total carbonate concentration is high from remineralisation of organic matter. Authigenic precipitation is enhanced by high pH, thus the alkalinity generated from the oxidation of

organic matter is a key driver of calcite or aragonite formation (Froelich et al. 1979; Abdelouas et al. 1999).

Precipitation of manganese carbonate is similar to that of calcium carbonate except that the concentration of dissolved manganese is more dynamic than that of Ca^{2+}. In oxic porewaters, Mn exists primarily as Mn(IV) in solid oxyhydroxides. Under reducing conditions, Mn oxides are reductively remobilised, causing the concentration of Mn^{2+} to increase with depth within the tailings/sediments (Froelich et al. 1979). At some depth, the concentrations of dissolved carbonate (which also increases with depth) and dissolved manganese may be sufficient to surpass the solubility product for certain manganous carbonate phases (Calvert and Pedersen, 1996).

Although there is evidence to suggest that radium can adsorb/coprecipitate with chemogenic aragonite, it is important to note that in general where carbonates form authigenically, they have very low trace metal concentrations. This is because metals will be preferentially precipitated by authigenic sulfides that precipitate under the same anoxic conditions. Thus, sorption onto or into authigenic carbonates is not a significant metal sink within the tailings pile.

5.1.4.2   Oxides of Fe and Mn

Studies by Markos (1979), Ritcey (1989), Tessier et al. (1996) and Martin et al. (2003) highlight the role of Fe and Mn oxyhydroxides as important scavengers of trace metals and radionuclides within uranium mill tailings. In the presence of dissolved oxygen, Fe and Mn, in their respective III and IV oxidation states, exist as solid phases which strongly sorb many trace metals. As the redox potential decreases, both Fe and Mn reduce to the II oxidation state, resulting in dissolution of their solid forms as described in Section 5.1.2.

In the tailings pile, reduction of Fe and Mn can occur as a result of successive depositional practices that eventually bury the solid oxides below the oxic/anoxic redox boundary. Upon reduction, Fe and Mn become highly soluble and can diffuse upward along a defined concentration gradient, toward the sediment-water interface where they re-precipitate in near-surface oxic sediment horizons forming Fe III and Mn IV oxides (Pederson et al. 1986; Pedersen et al. 1993; Martin et al. 2003). Since Fe and Mn oxides are efficient in adsorbing and co-precipitating a broad range of metal ions, these oxides provide an effective "metal scavenging" mechanism that inhibits the release of dissolved metals in the water column

(Thornber, 1992; Tessier et al. 1996). These processes are examined in conjunction with the sediment/porewater data to determine the reactivity of the tailings with respect to metal release.

For natural sediments, this cycle of reductive dissolution at suboxic depths, upward migration and reprecipitation (with commensurate scavenging of trace metals from the dissolved phase) in oxygenated sediments, can result in significant accumulations of Fe and Mn oxides in surface sediments (Pederson et al. 1993). In anthropogenic sediments such as tailings, these processes are also evident but not initially apparent due to the progressive and rapid deposition of tailings into the impoundment area. As will be demonstrated later, Fe and Mn oxides play a key role in controlling the solid state speciation, and hence, solubility of radionuclides and trace metals within the tailings pile.

5.1.4.3   Sulfides

Reduced sulfur is ubiquitous in both natural and tailings sediments and is capable of precipitating or adsorbing a wide range of trace metals (e.g. Fe, Cd, Zn, Mo and Cu) (Jean and Bancroft, 1986). The most abundant authigenic sulfides are those of iron: FeS (pyrrhotite, mackinawite, greigite) and FeS_2 (pyrite, marcasite), reflecting both the abundance of iron and its reactivity towards reduced sulfur. Studies on sulfide and sulfate in Ranger tailings by Fordham and Beech (1989) and Fordham et al. (1993) did not find evidence of authigenic sulfides in cores sampled from the tailings surface to a depth of 11 m, although they did observe primary metal sulfides such as pyrite, galena and chalcopyrite. Authigenic sulfides were not observed in the mineralogical survey of the tailings cores; however, as will be further discussed in Chapter 6, mackinawite ($FeS_{0.9}$) did form during the kinetic column leach tests.

Understanding the mechanisms governing the formation of authigenic sulfides is critical in planning for the safe closure of the tailings repository as the microbial processes active within such an environment could promote reduction of large amounts of sulfate to more insoluble metal sulfides (Table 5.1). In the long term and following progressive de-watering of the tailings, sulfide oxidation may occur leading to increased acidity and release of radionuclides and trace metals from the tailings repository.

5.2.   Tailings Texture, Mineralogy and Geochemistry

Of the 45 cores recovered from the tailings impoundment, six were selected as best representing the various lithogenic and authigenic phases observed along the 1 km long N-S sampling transect (see Figure 4.1). These cores, as shown in Figure 5.3, were subjected to a detailed physical, mineralogical, geochemical and analytical program, the results of which are presented and discussed in the following sections. Bulk phase mineralogy and geochemistry were determined on the remaining 39 cores to augment the findings of the aforementioned studies. Detailed results of the mineralogical, geochemical and hydrochemical studies are summarised in Appendix 2.

5.2.1   Tailings Texture

Visual examination of the six representative cores (Figure 5.3) clearly shows alternating layers comprising very distinctive material fractions.

SITE 4	DEPTH (m)	PHASE DESCRIPTION	TEST PROGRAM
	11.0 — 11.1	Fine grain (silt) lithogenic tailings	n/a
	11.1 — 11.2	As above	n/a
	11.2 — 11.3	As above	n/a
	Sampled (11.38) 11.3 — 11.4	As above	Submitted for detailed particle size, mineralogical, morphological and geochemical characterisation
	11.4 — 11.5	As above	n/a

Figure 5.3:   Tailings texture and phase descriptions

* Not Analysed

SITE 5	DEPTH (m)	PHASE DESCRIPTION	TEST PROGRAM
	7.0 ... 7.1	Fine grain (silt) lithogenic tailings with interspersed authigenic phases	n/a
	Sampled (7.11) ... 7.2	Authigenic FeOx and gypsum phases	Submitted for detailed particle size, mineralogical, morphological and geochemical characterisation
	7.3	Coarse grain (sand) lithogenic tailings	n/a
	7.4	Fine grain (silt) lithogenic tailings	
	7.5	Authigenic FeOx and gypsum phases overlying fine grain (silt) lithogenic tailings	n/a

SITE 5	DEPTH (m)	PHASE DESCRIPTION	TEST PROGRAM
	10.0 ... 10.1	Predominantly fine grain (silt) lithogenic tailings	n/a
	10.2	As above	n/a
	10.3	Authigenic FeOx in a matrix of fine grain tailings	n/a
	Sampled (10.34) ... 10.4	Predominantly fine grain (silt) lithogenic tailings	Submitted for detailed particle size, mineralogical, morphological and geochemical characterisation
	10.5	As above	n/a

Figure 5.3 – cont'd

SITE 5		DEPTH (m)	PHASE DESCRIPTION	TEST PROGRAM
		11.0	Predominantly coarse grain (sand) lithogenic tailings	n/a
		11.1		
		Sampled (11.13)	Authigenic phases Gypsum, FeOx and MnOx	Submitted for detailed particle size, mineralogical, morphological and geochemical characterisation
		11.2		
			Predominantly coarse grain (sand) lithogenic tailings	n/a
		11.3		
			As above	n/a
		11.4		
			As above	n/a
		11.5		

SITE 6		DEPTH (m)	PHASE DESCRIPTION	TEST PROGRAM
		5.0	Coarse grain (sand) lithogenic tailings	n/a
		5.1		
			As above with interbedded fine grain tailings	n/a
		5.2		
			Coarse grain (sand) lithogenic tailings with interbedded fine grain (silt) lithogenic tailings	n/a
		5.3		
			Authigenic phase Gypsum and FeOx underlain by coarse grain tailings	n/a
		5.4		
		Sampled (5.45)	Coarse grain (sand) lithogenic tailings with interbedded fine grain (silt) lithogenic tailings	Submitted for detailed particle size, mineralogical, morphological and geochemical characterisation
		5.5		

Figure 5.3 – cont'd

SITE 6	DEPTH (m)	PHASE DESCRIPTION	TEST PROGRAM
	12.0 12.1	Fine grain (silt) lithogenic tailings	n/a
	   12.2	As above	n/a
	   12.3	As above	n/a
	Sampled (12.36) 12.4	As above	Submitted for detailed particle size, mineralogical, morphological and geochemical characterisation.
	   12.5	As above	n/a

Figure 5.3 – cont'd

In conjunction with the results of the particle size analysis (Figure 5.4), it can be demonstrated that the tailings are spatially variable, comprising a complex heterogeneous mixture of sands, silts and authigenic phases. Of these fractions, only the silts (Sites 4 (11.38 m), 5 (10.34 m) and 6 (12.36 m)) and authigenic phases (Site 5, 7.11 m and 11.13 m samples) show a very fine depositional texture with between 50 to 90% of these material fractions passing through 20 µm. In contrast, the coarse grain tailings (Site 6, 5.45 m) display a mass distribution where less than 10% passes through 10 µm.

Visual examination of the remaining 39 cores, showed that Sites 3 and 5 located within close proximity (150 to 200 m) to the dam wall contained a higher proportion of the coarse sand fraction relative to those Sites (4, 6 and 9) located toward the centre of the impoundment. This qualitative observation implies that textural sorting strongly influences the nature of sedimentation in the tailings impoundment. This phenomenon is not unusual in tailings impoundments in which suspended solids in a high energy environment (i.e. tailings pipeline) enter low energy, quiescent waters (i.e. tailings pond), causing the coarse and more dense fractions to settle out closer to the input point than the finer fractions.
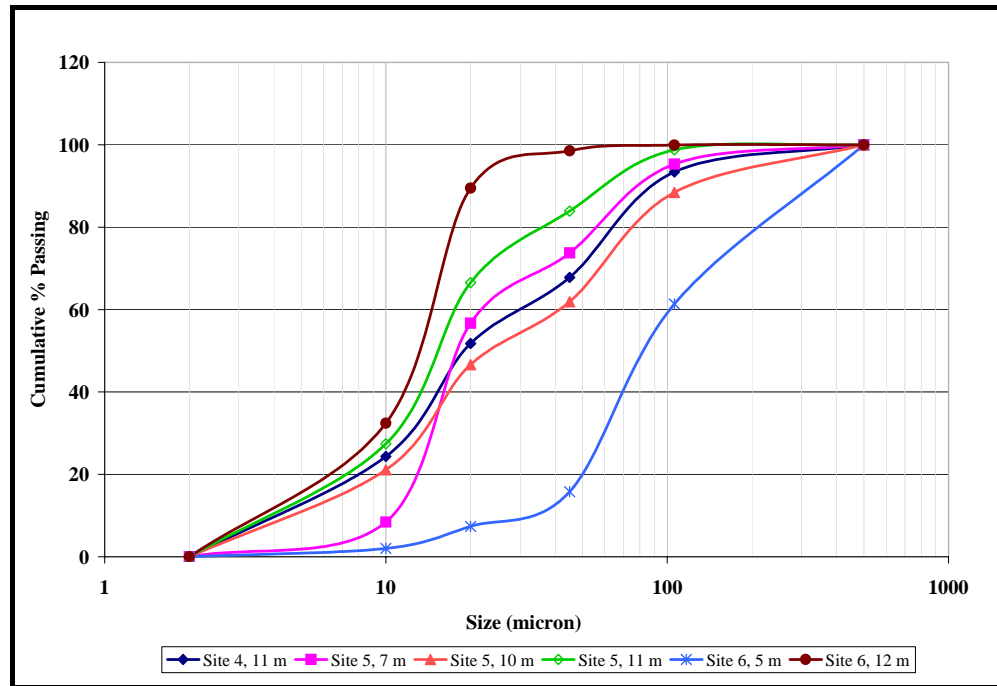
Figure 5.4:   Tailings size distribution

Textural sorting also impacts on sediment mineralogy and tailings permeability/hydrology (Calvert, 1976). Both of these parameters influence the partitioning, mobility and mass transport of radionuclides and trace metals within the tailings pile.

In this context, the mineralogy and geochemistry of the tailings solids were assessed in relation to the following material fractions:

- Bulk phase – composite sample taken over the entire length of the tailings core.

- Coarse sand fraction (> 62 µm), representative sample obtained from the Site 6 core, at a depth of 5.45 m.

- Silt fraction (2 µm – 62 µm), representative samples obtained from the Sites 4 , 5 and 6 cores at depths 11.38 m, 10.34 m and 12.36 m, respectively.

- Authigenic phases (< 2 µm), representative sample obtained from site 5 core at depths 7.11 m and 11.13 m.

These results are presented and discussed in Sections 5.2.2 and 5.2.3.

5.2.2   Tailings Mineralogy and Morphology

5.2.2.1   Bulk Phase Mineralogy

X-ray diffraction analyses of composite samples obtained from each of the 45 (0.5 m) cores are summarised in Table 5.2.

Table 5.2:   Mineralogical composition of composite samples obtained from 0.5 m tailings cores

Mineral	*Chemical Composition	Abundance (% wt/wt)
Mg-Chlorite	$Mg_3Fe_2Al_2Si_3O_{10}(OH)_8$	> 60%, sum of phases co-dominant with quartz (major phase)
Quartz	SiO_2	as above (major phase)
Muscovite	$K_2Al_4[Si_6Al_2O_2](OH,F)_4$	5 - 20% (minor phase)
Hematite	Fe_2O_3	5 - 20% (minor phase)
Gypsum	$CaSO_4 \bullet 2H_2O$	5 - 20% (minor phase)
Magnesite	$MgCO_3$	< 5% trace
Kaolinite	$Al_2Si_2O_5(OH)_4$	< 5% trace

* Source: Deer et al. (1966); Nesbitt and Jambor (1998)

Chlorite and quartz are the only major rock forming minerals and common to all sample sites along the N-S transect. Muscovite, hematite and gypsum are present in varying but minor amounts. Fine white mica (sericite) is also present and was presumably formed as an alteration product of K-feldspars (Ewers and Ferguson, 1980). Primary hematite present in the tailings is associated with the uranium orebody as a chlorite alteration product although, authigenic iron minerals (amorphous oxy-hydroxides) are also present in the tailings, as will be discussed in subsequent sections.

The presence of trace magnesite is indicative of post depositional or diagenetic processes as carbonate minerals associated with the uranium ore are consumed during the acid leach process. Upon lime neutralisation dissolved Ca (previously associated with calcite, dolomite or magnesite) precipitates as gypsum. Kaolinite is a mineralogical indicator of chlorite and biotite alteration. These mechanisms are discussed in the following section and Chapter 6 as they are central to the long term geochemical stability of the tailings pile.

5.2.2.2   Mineralogy and Morphology of Selected Size Fractions and Phases

To assess the influence of textural sorting on sediment mineralogy within the tailings pile, quantitative scanning electron microscopy (QEMSEM) was used to determine the distribution of the major, minor and trace mineral assemblages as a function of grain size. Figures 5.5 to 5.13 show the distribution of gypsum, Fe/Mn oxides, magnesium minerals, uranium oxides, pyrite, chlorite, mica, quartz and Al-silicate phases, respectively.
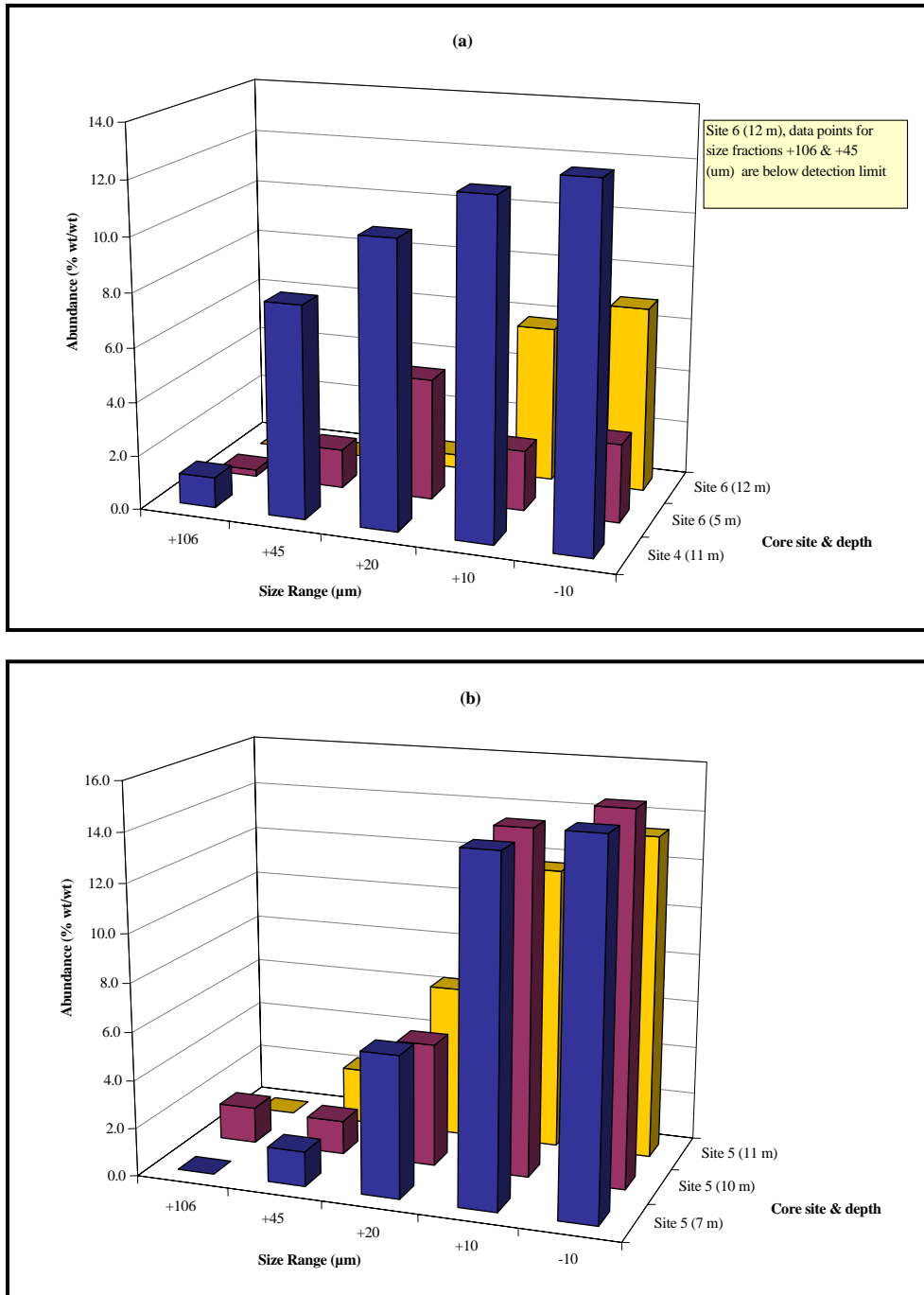
Figure 5.5:   Gypsum distribution for (a) Sites 4 & 6 and (b) Site 5

(a)

(b)
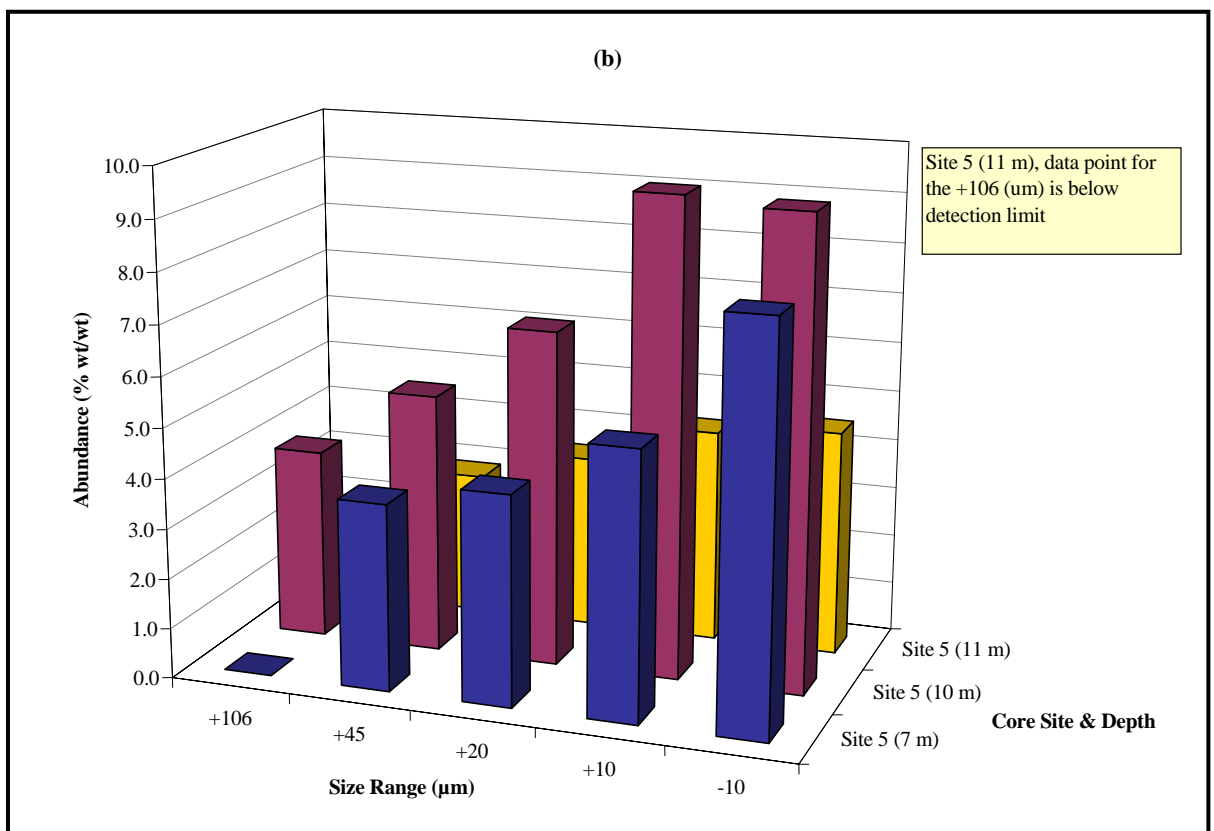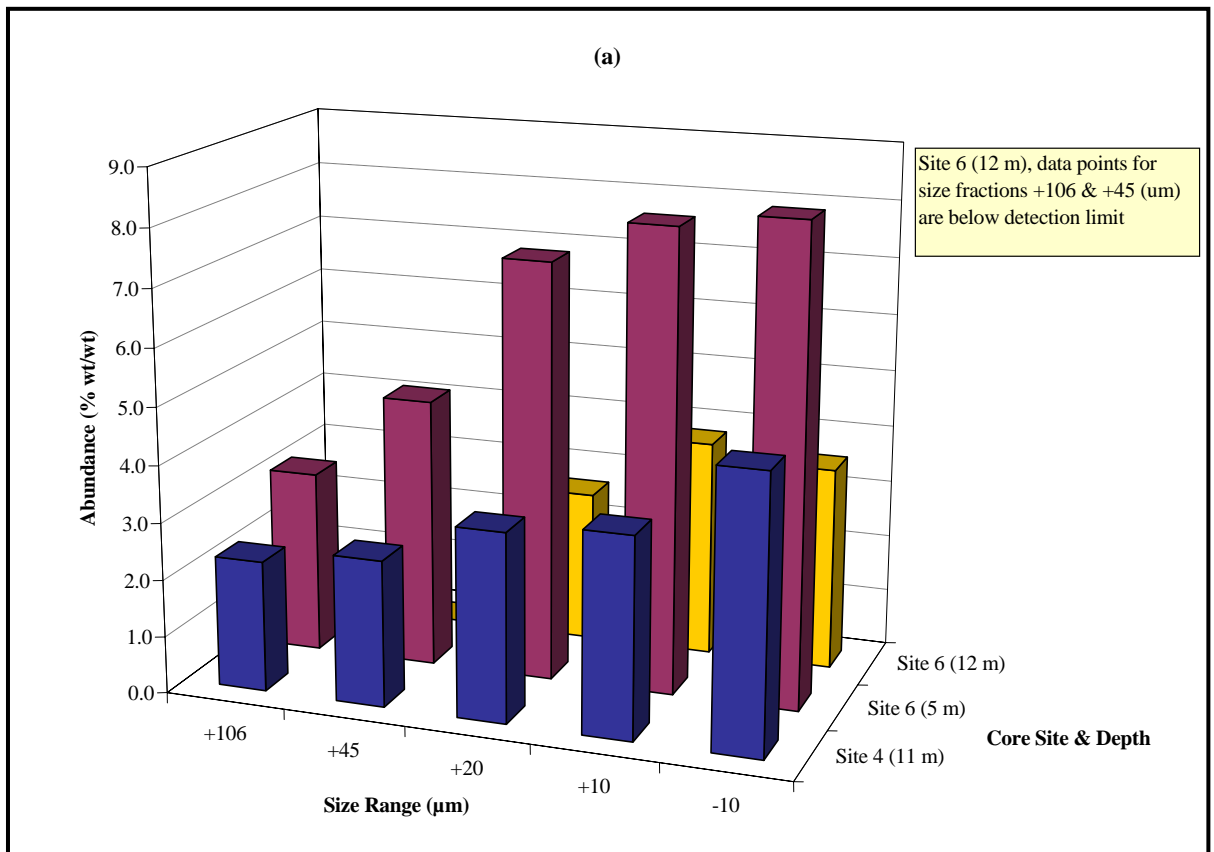
Figure 5.6:   Iron oxide distribution for (a) Sites 4 & 6 and (b) Site 5

(a)

(b)
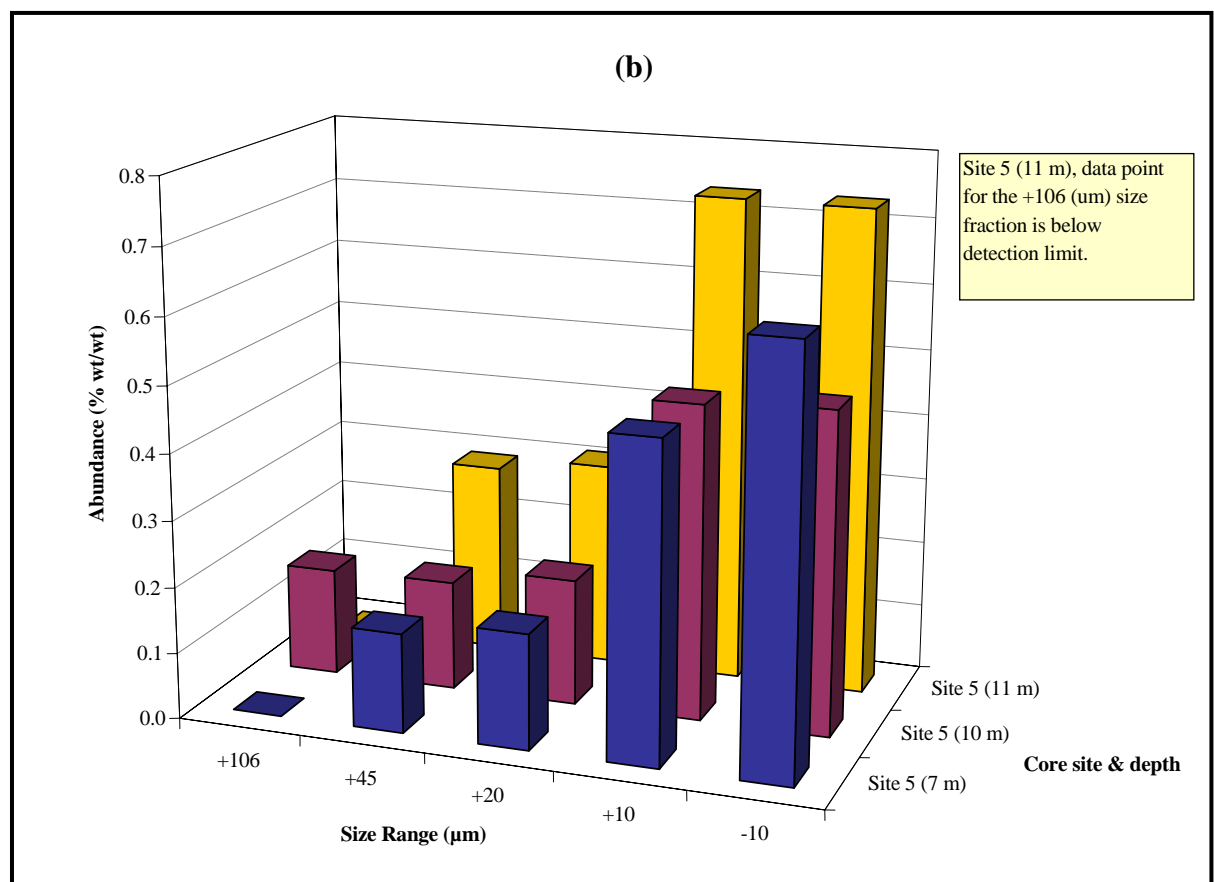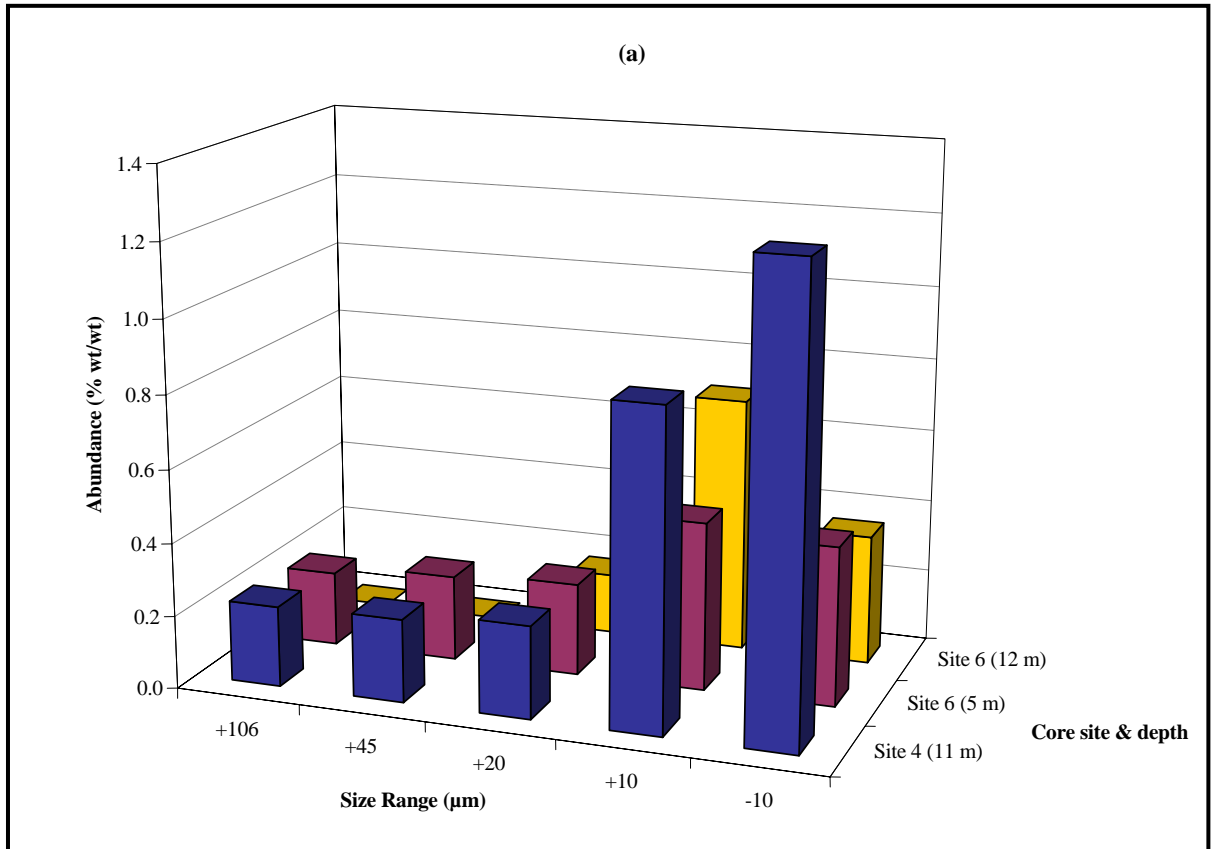
Figure 5.7:   Manganese oxide distribution for (a) Sites 4 & 6 and (b) Site 5

(a)

(b)
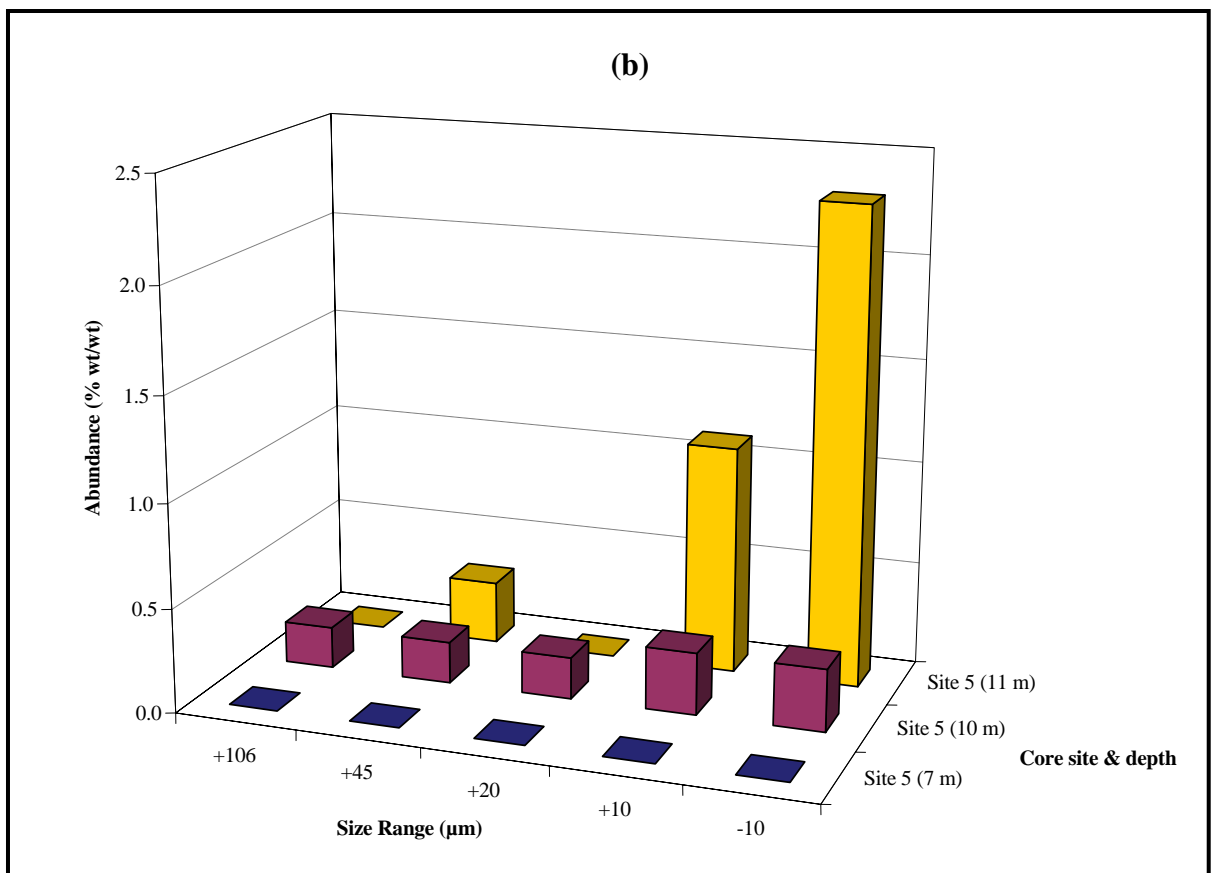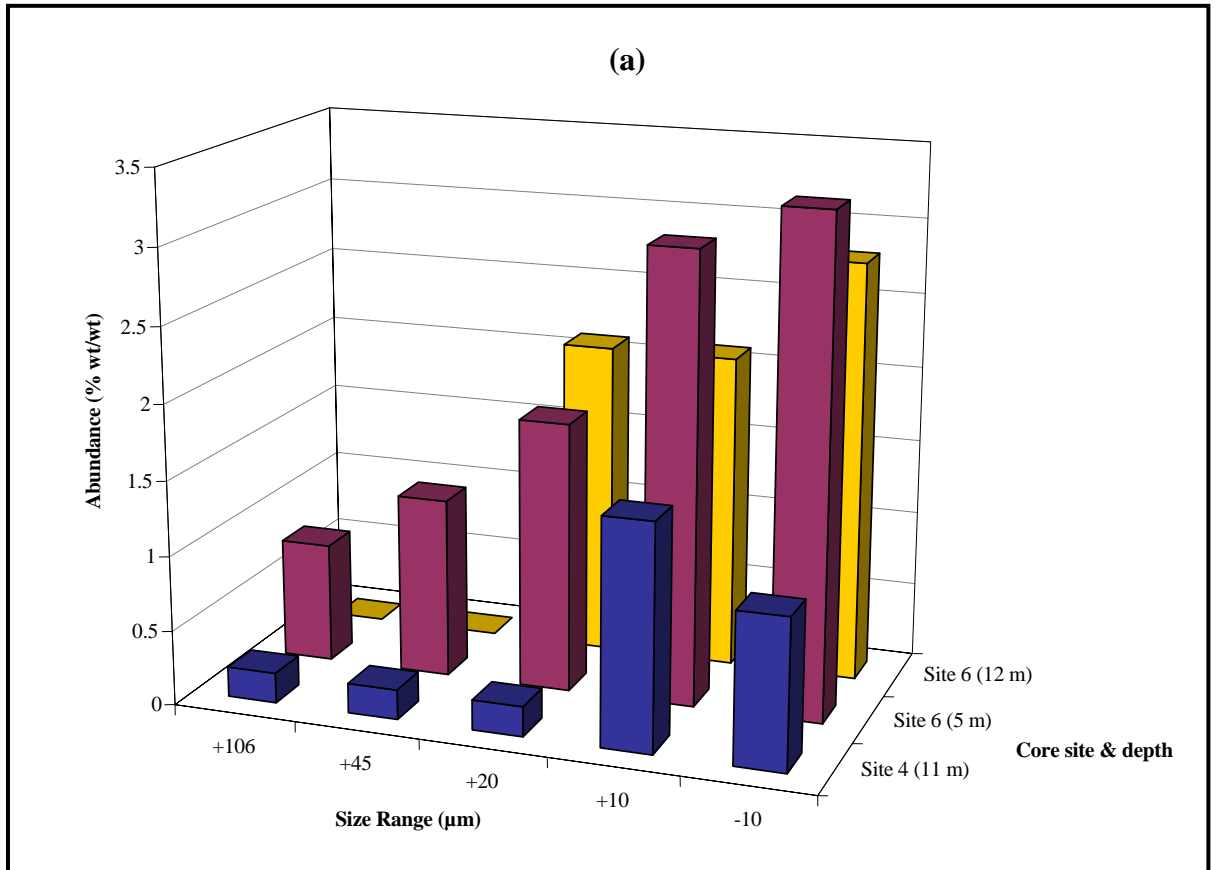
Figure 5.8:   Magnesium phase distribution for (a) Sites 4 & 6 and (b) Site 5
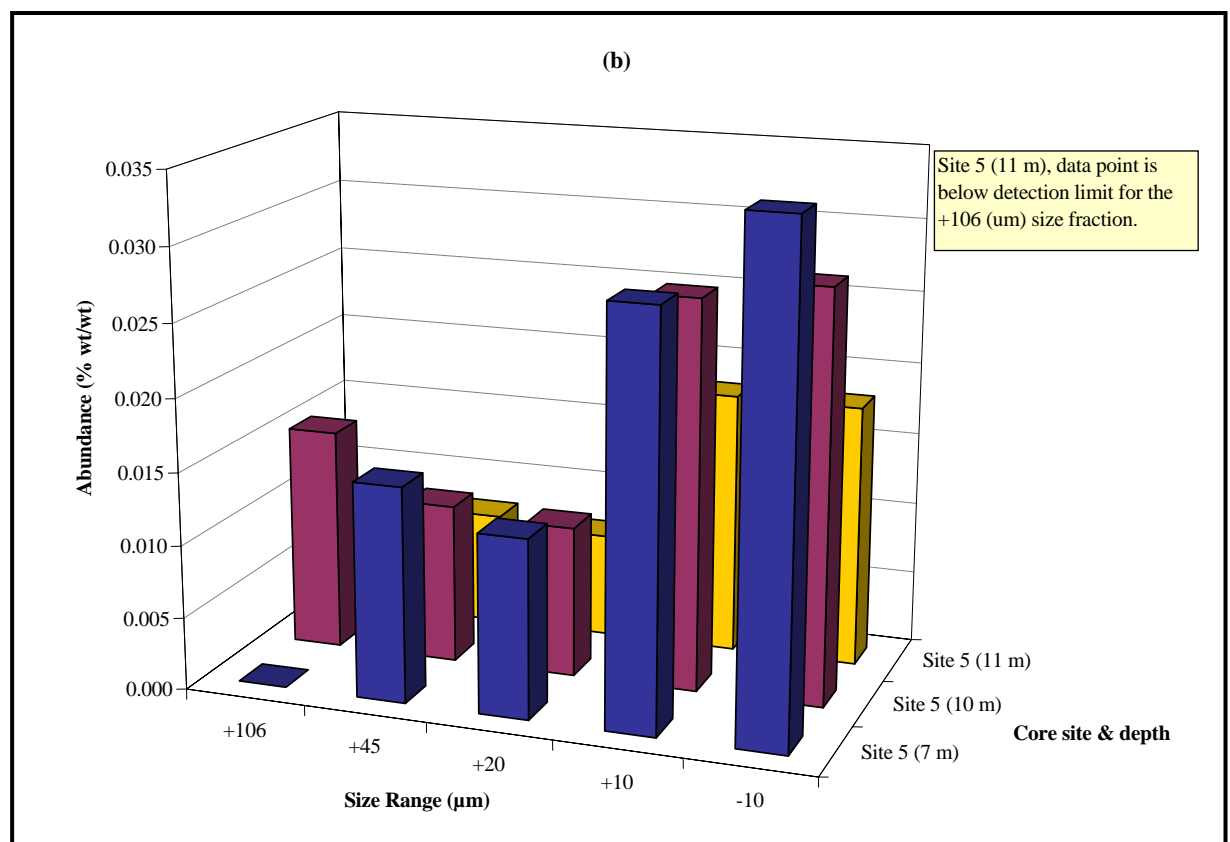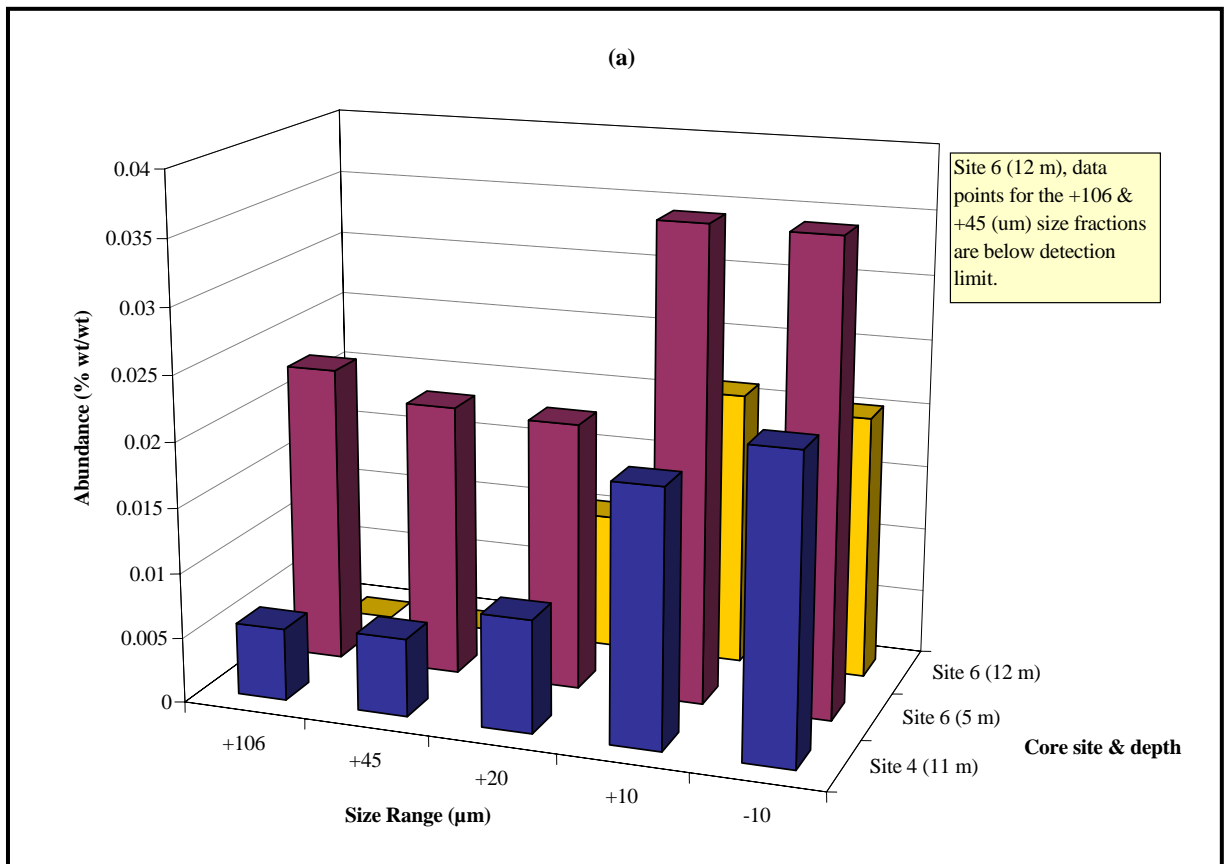
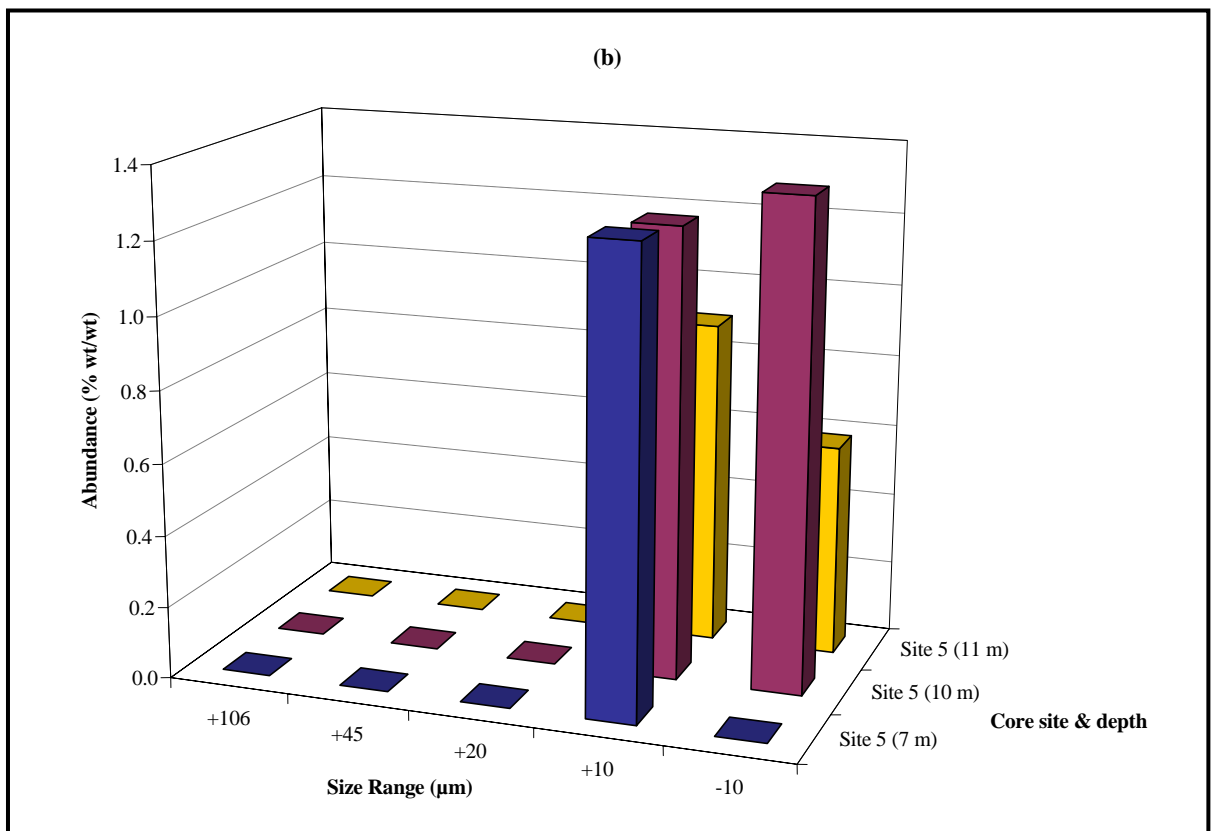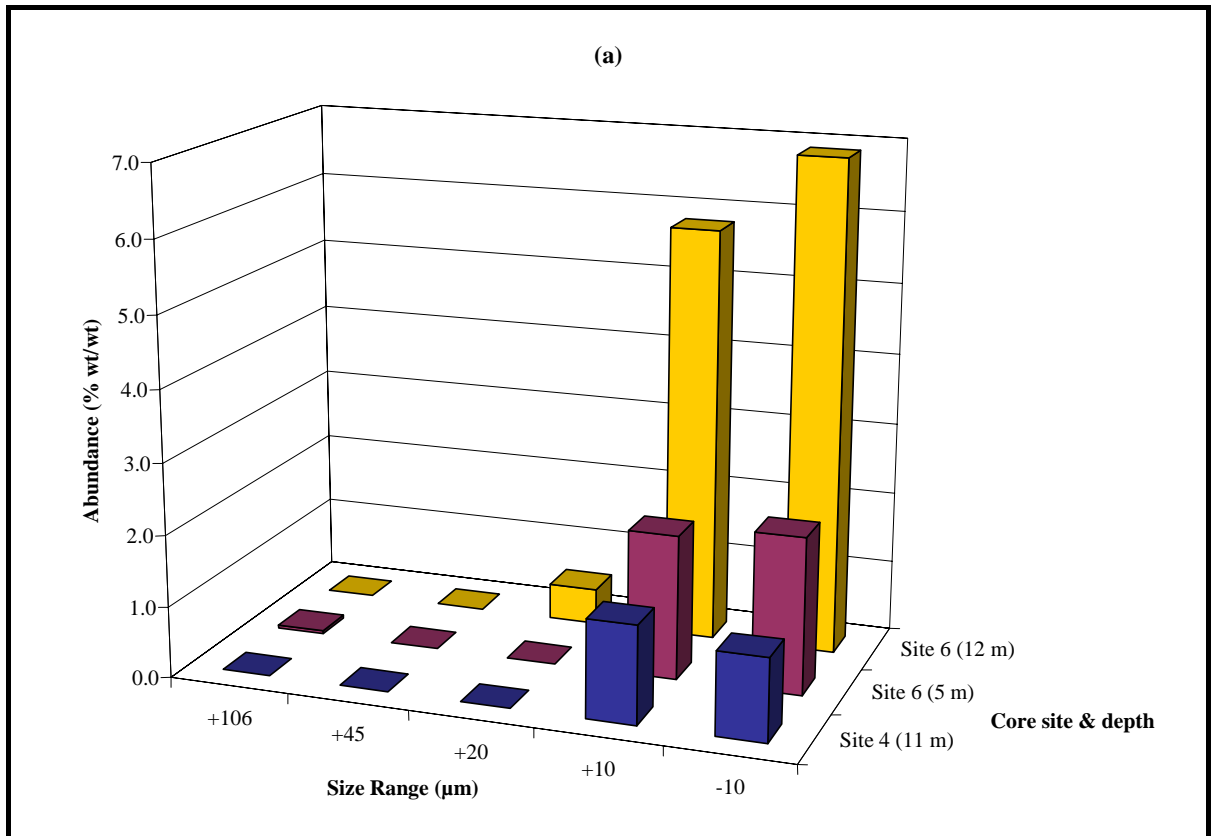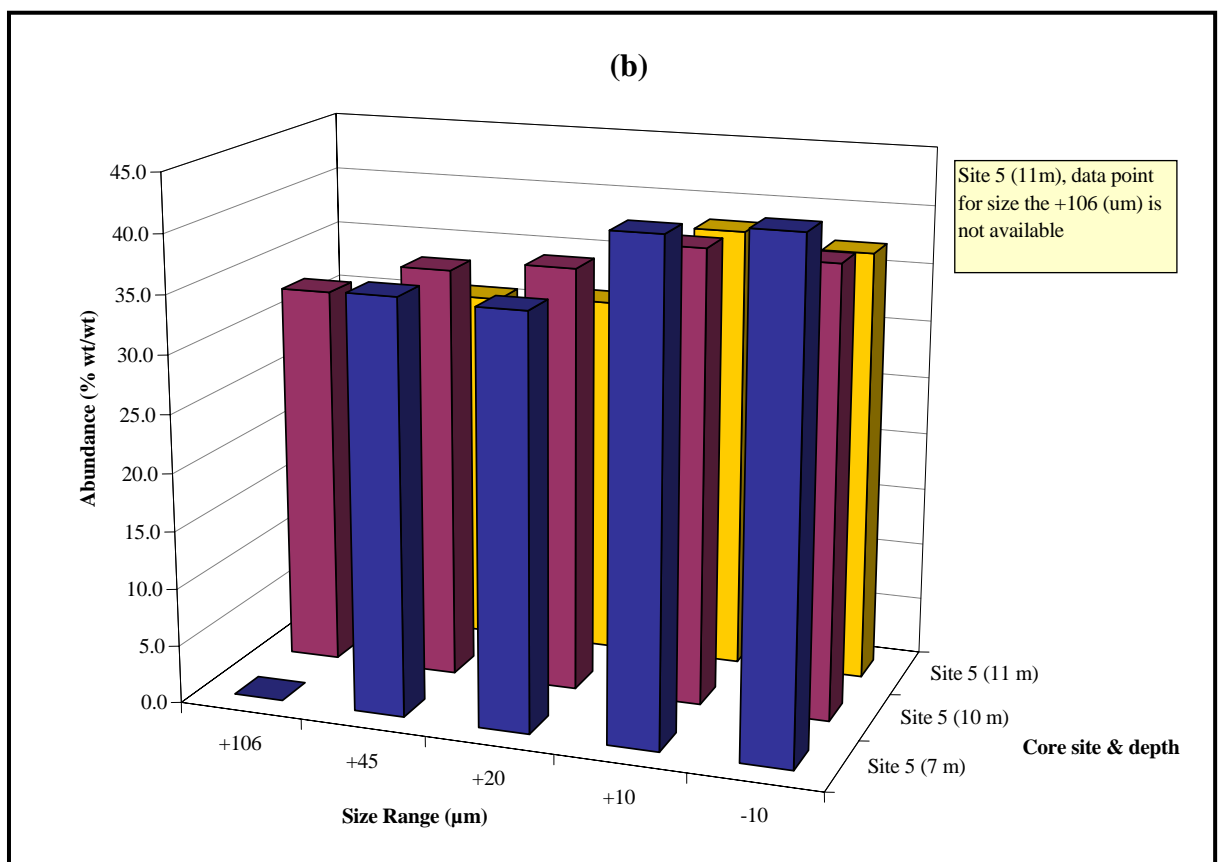**Figure 5.9:   Uranium phase distribution for (a) Sites 4 & 6 and (b) Site 5**

(a)

(b)

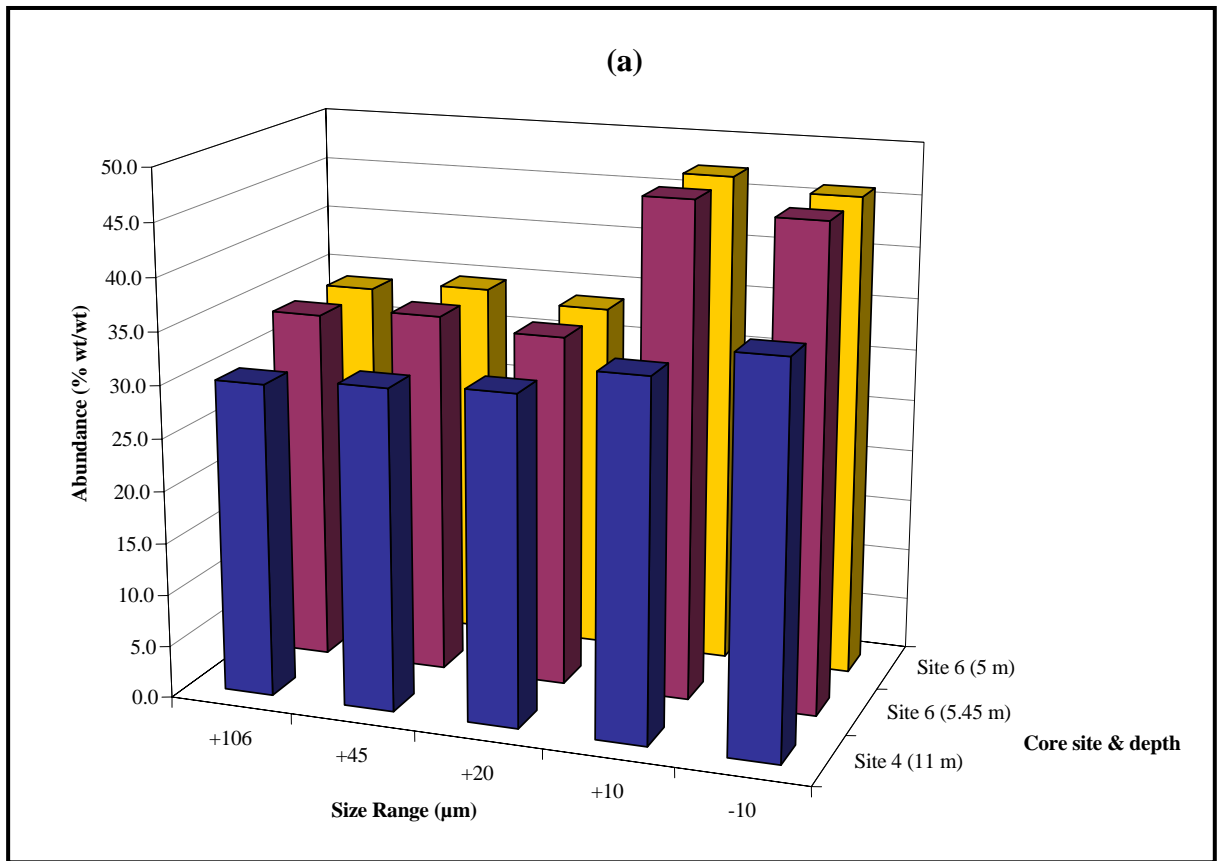**Figure 5.10:   Pyrite distribution for (a) Sites 4 & 6 and (b) Site 5**

(a)

(b)

Site 5 (11m), data point
for size the +106 (um) is
not available

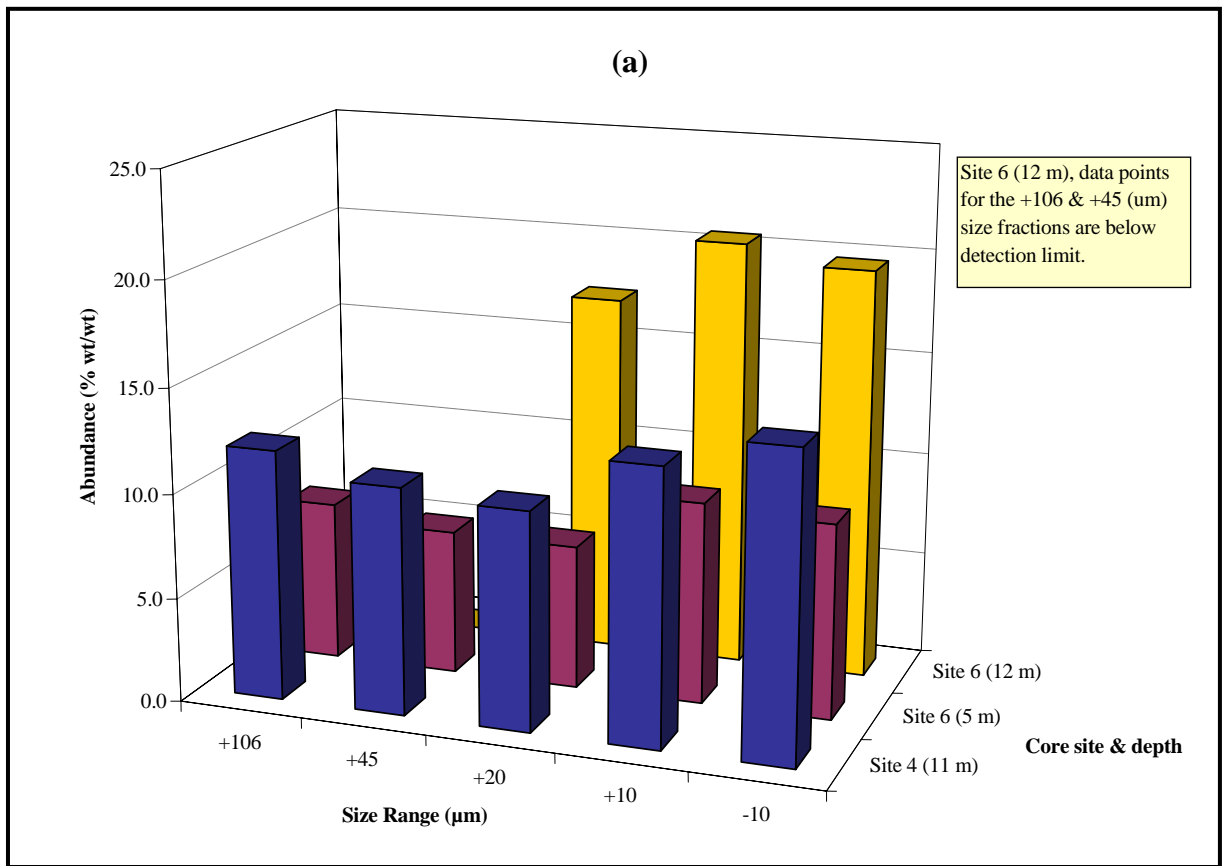**Figure 5.11(a):   Chlorite distribution for (a) Sites 4 & 6 and (b) Site 5**

(a)

Site 6 (12 m), data points for the +106 & +45 (um) size fractions are below detection limit.

(b)

Site 5 (11 m), data point for the +106 (um) size fraction is below detection limit.
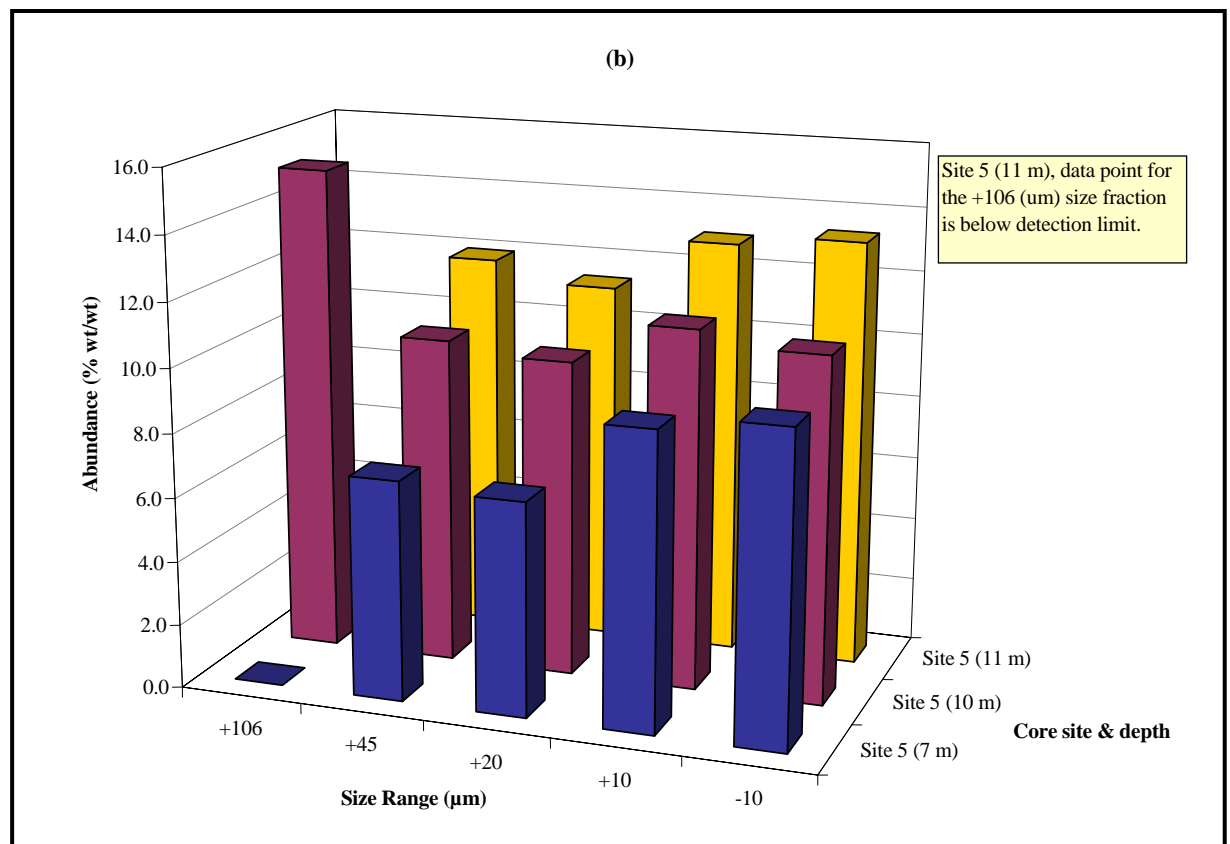
Figure 5.11 (b):   Mica distribution for (a) Sites 4 & 6 and (b) Site 5
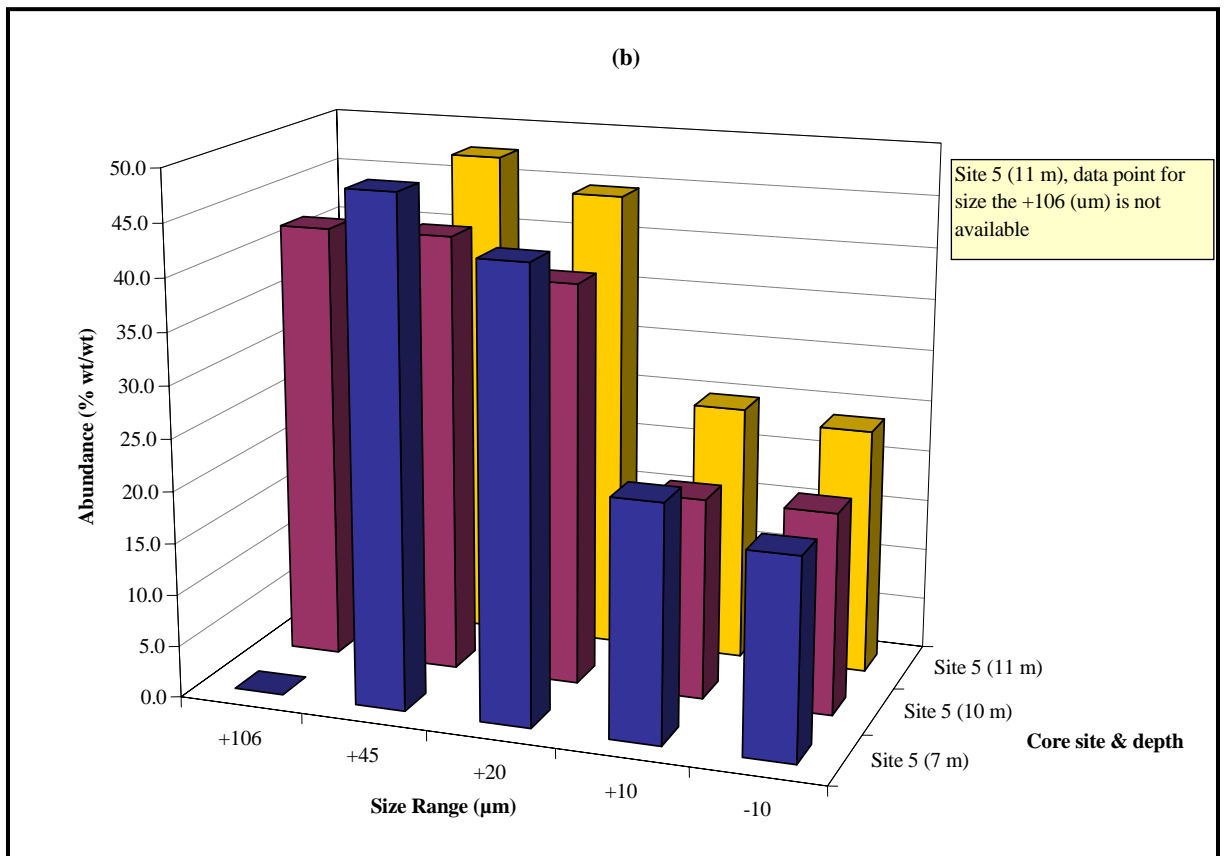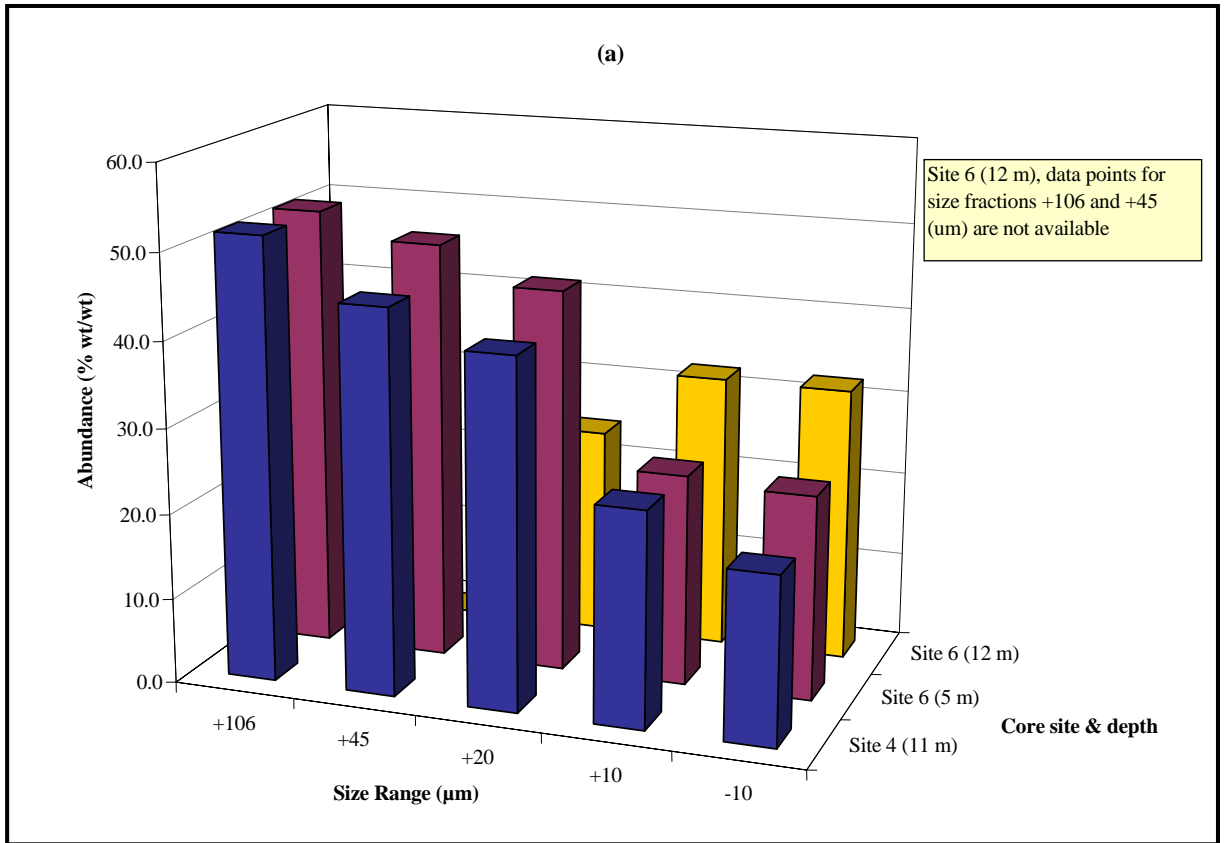
(a)

(b)

Figure 5.12:   Quartz distribution for (a) Sites 4 & 6 and (b) Site 5
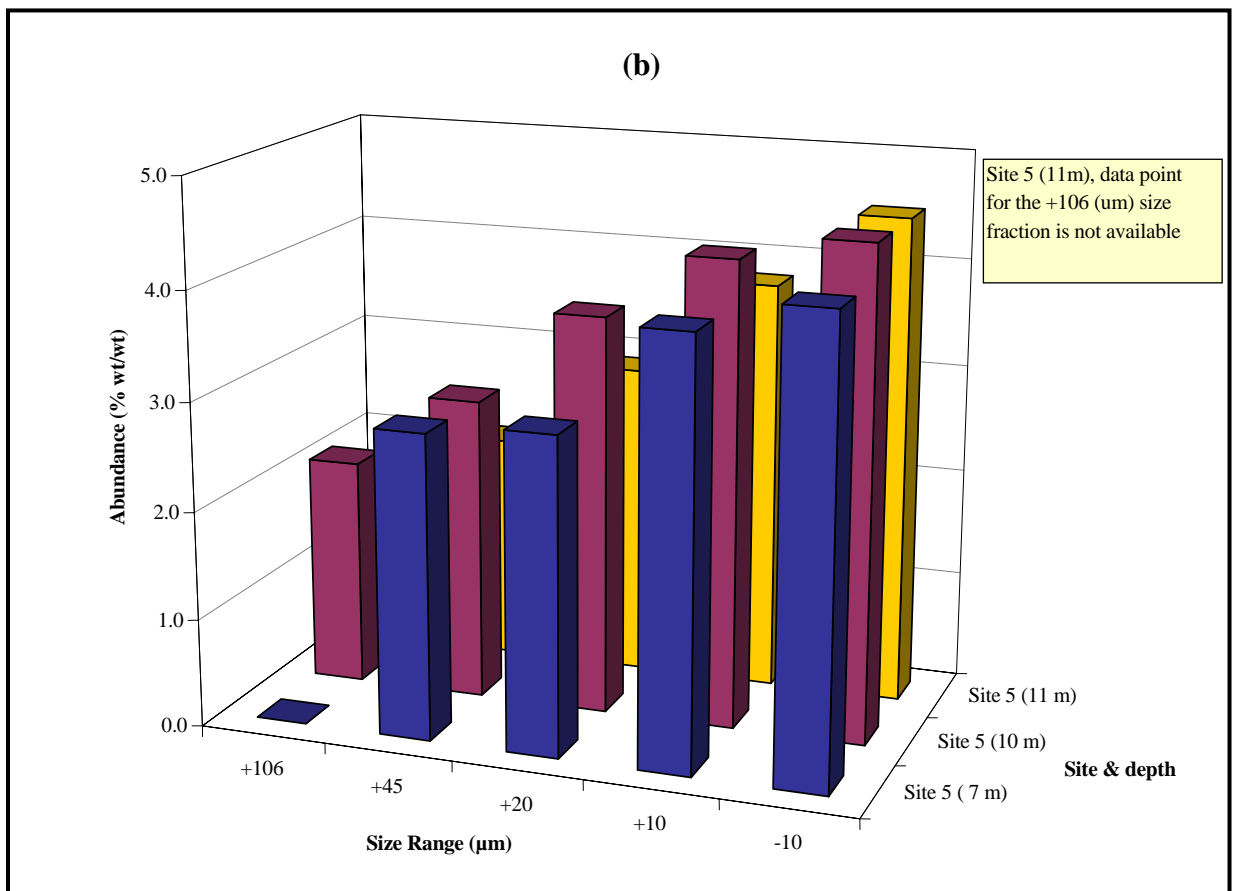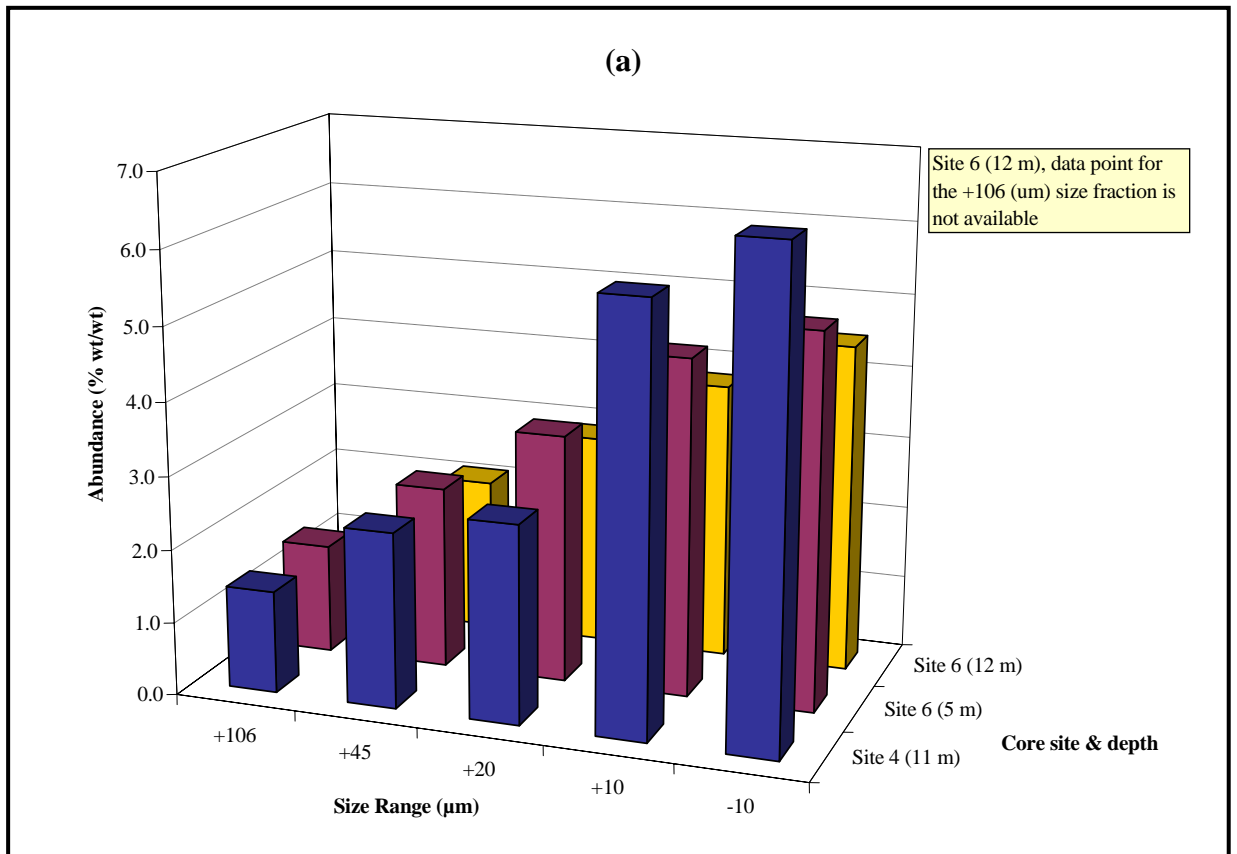
(a)

(b)

Figure 5.13: Al-Silicate distribution for (a) Sites 4 & 6 and (b) Site 5

As shown in Figures 5.5, 5.6, 5.7, 5.8 and 5.9, secondary minerals such as gypsum (up to 14%), iron oxides (up to 9%), manganese oxides (up to 1%), magnesium phases (carbonates/sulfates) (2%) and uranium phases (up to 0.035%) are typically enriched in the < 20 µm size fraction irrespective of depth or location within the tailings pile. These minerals presumably either form following lime neutralisation as described in Section 5.1.1 or as a result of diagenetic processes. Pyrite (Figure 5.10) is predominantly associated with the fine grained size fractions (< 20 µm) and occurs as an authigenic phase arising from the microbial conversion of sulfate to sulfide (Fordham et al. 1993). Primary pyrite is associated with the > 20 µm size fractions. This was confirmed by SEM-EDX and is further discussed in Section 6.3.2.

Uranium oxide minerals (Figure 5.9) are generally enriched up to 0.035% in the < 20 µm fractions diminishing to less than 0.025% in the coarse tailings fractions (> 45 µm). These trends in conjunction with SEM images (discussed below), suggest that uranium minerals exist as both primary and secondary oxides with the latter being mainly associated with the < 20 µm material fractions.

Chlorite, and to a lesser extent mica (Figures 5.11(a) and (b)), are ubiquitous with relatively uniform abundances over the tailings depth profile and particle size range. In contrast, the mass distribution of quartz (Figure 5.12) tends to be higher in the coarse silt/sand size range (> 45 µm) than in the finer size fractions.

In the case of the coarse silt/sand tailings fraction (> 45 µm), the abundance of secondary minerals significantly diminishes. Primary hematite (Figure 5.6) is also present in minor amounts and is presumably present as a chlorite alteration product (Ewers and Ferguson, 1980).

Aluminium silicate phases (Figure 5.13) predominately in the form of kaolinite are present in trace amounts (< 5%) with the highest abundances being associated with the < 10 µm size fraction. These results are consistent with those of Savory (1994) who reported kaolinite abundances on the order of 3.3% in the weathered zone of the Ranger #1 orebody.

Kaolinite is principally formed by hydrothermal alteration or weathering of phyllosilicates such as chlorite and biotite (Deer et al. 1966). As uranium mineralization is intimately associated with massive chlorite, knowledge of chlorite weathering processes are key to understanding the redistribution of cations (Mg, Al and Fe) and radionuclides within the tailings pile. Studies by

Airey (1986) and Murakami et al. (1992) at the nearby Koongara uranium deposit (20 km south of Ranger) described the weathering sequence as the initial conversion of chlorite to vermiculite ($(Mg,Fe,Al)_3(Si,Al)_4O_{10}(OH)_2 \cdot 4H_2O$), followed by the decomposition of vermiculite to kaolinite ($Al_2Si_2O_5(OH)_4$). Reaction by-products include the release of Mg^{2+} ions and the formation of ferrihydrite ($Fe(OH)_3$) and amorphous silica phases. The study also found that biotite is subjected to the same weathering process. Based on the thickness of the chlorite/kaolinite weathering profile and the geological history of the Koongara site, Airey (1986) estimated the reaction time of chlorite to kaolinite at around 1 to 3 My.

In a stable geological environment such as the Ranger and Koongara ore-bodies, chlorite appears to be a relatively unreactive mineral. However, based on studies by Williams (1982), Lapakko (1987), Fordham et al. (1993) and Nesbitt and Jambor (1998), chlorite will react with the acid produced from the oxidation of metal sulfides. The reaction mechanism is similar to the weathering sequence described by Airey (1986) and Murakami et al. (1992). But as will be shown in Chapter 6, where the reaction kinetics are much faster under acidic conditions, chlorite weathering processes were observed to occur within the 520 day leaching period of the column experiment. Such conditions are present in the tailings pile and are further examined in Chapter 6 and modelled in Chapter 7.

Mineral morphology and chemical composition of the various tailings minerals were assessed by SEM-EDX microanalysis to determine the degree of weathering of primary minerals and the nature and distribution of secondary mineral assemblages. SEM field views typical of coarse, silt and fresh precipitate fractions are shown in Figures 5.14 to 5.20.

For the coarse tailings function (Figure 5.14), quartz is present as sharply angular fragments up to 50 µm in size. Hematite is also present being formed as an alteration product of chlorite. Chlorite occurs as large crystals greater than 80 µm in length. The chemical composition of several chlorites measured by EDX (Table 5.3) identified only the magnesium rich form. These results are consistent with the chlorite analyses reported by Deer et al. (1966) and studies by Edis et al. (1992) and Nesbitt and Jambor (1998) which proposed a generalised formula for Mg rich chlorite as being $Mg_3Fe_2Al_2Si_3O_{10}(OH)_8$.

In contrast to the coarse tailings, chlorite in the silt size fraction (Figure 5.15) occurs as pervasive microaggregates or a fine grained groundmass.

Table 5.3: Energy dispersive X-Ray analyses of chlorite in various tailings samples

Site Depth	Tailings Type	SiO_2 (wt%)	Al_2O_3 (wt%)	MgO (wt%)	FeO (wt%)	TiO_2 (wt%)	MnO (wt%)	K_2O (wt%)	Na_2O (wt%)	CaO (wt%)	Total (wt%)
Site 6, 5.45 m	Sand	30.8	22.7	23.2	11.6	0.4	0.1	0.2	0.1	0.0	89.1
Site 5, 10.34 m	Silt	27.6	22.4	24.3	12.1	0.2	0.1	0.1	0.2	0.0	87
Site 5, 7.11 m	Clay	28.9	23	24.8	12.5	0.1	0.1	0.1	0.2	0.0	89.7
Deer et al. (1966) Mg rich chlorite	Ave. n=3	25.5	22.7	21	15.7	0.55	0.18	0.06	0.17	0.4	86

Note: remaining mass balance is due to water of hydration (H_2O - 11 to 13%)
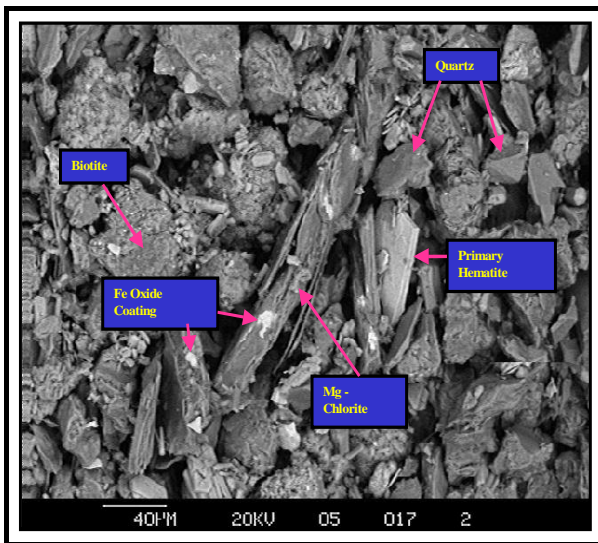

Figure 5.14:   SEM Field View of Coarse Grain Tailings - Sample site 6 - depth 5.45 m (backscatter mode)
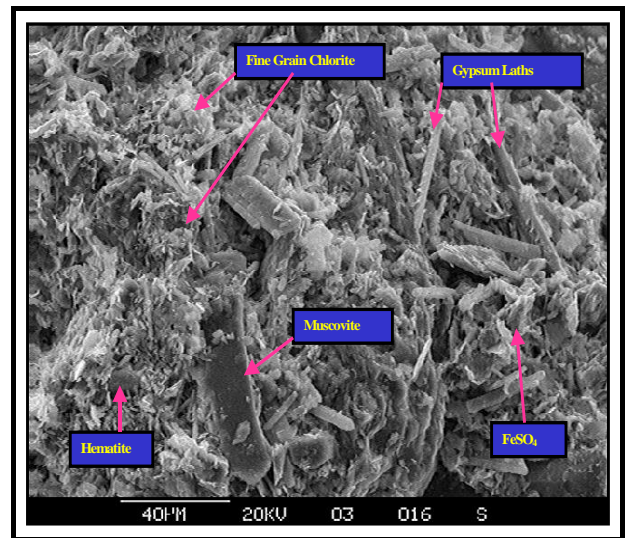

Figure 5.15: SEM field view of silt size tailings Site 4 (11.38 m)

Muscovite is present as large (> 40 μm) tabular flakes with a chemical composition (Table 5.4) close to that of pure muscovite ($KAl_2(AlSi_3O_{10})$ $(OH)_2$).

Table 5.4:   Energy dispersive X-Ray analyses of muscovite, Site 4 (11.38 m)

SiO_2 (wt%)	Al_2O_3 (wt%)	MgO (wt%)	FeO (wt%)	TiO_2 (wt%)	MnO (wt%)	K_2O (wt%)	Na_2O (wt%)	CaO (wt%)	Total (wt%)
45.5	36.7	1.4	2.1	0.5	0.1	10.4	0.4	0.0	97.1

Figure 5.16:   Groundmass of fine grained chlorite in the presence of gypsum laths Site 4 (11.38 m)

In both the coarse and silt fractions, muscovite and chlorite are present in a relatively unweathered state. The unreactive nature of these minerals, particularly during the harsh conditions of the acid leach extraction process, is indicative of their geochemical stability. The inert nature of these minerals is highly desirable from a closure perspective, as trace metals and radionuclides occluded within these minerals are unlikely to be released into the environment.

Gypsum ($CaSO_4 \cdot 2H_2O$) dominates the silt fraction as large (50 µm) euhedral crystals or laths (Figures 5.15 and 5.16). Gypsum shows very little variation in chemical composition and although there are other hydrated forms, bassanite ($CaSO_4 \cdot 0.5H_2O$) and anhydrite ($CaSO_4$), these minerals were not identified by XRD or SEM-EDX analysis. Other alkaline earth sulfates identified by SEM-EDX (Figure 5.17) include microaggregates of barite ($BaSO_4$). The

presence of barite is geochemically significant as this phase has a propensity to co-precipitate radium-226, thus reducing its mobility within the water column.
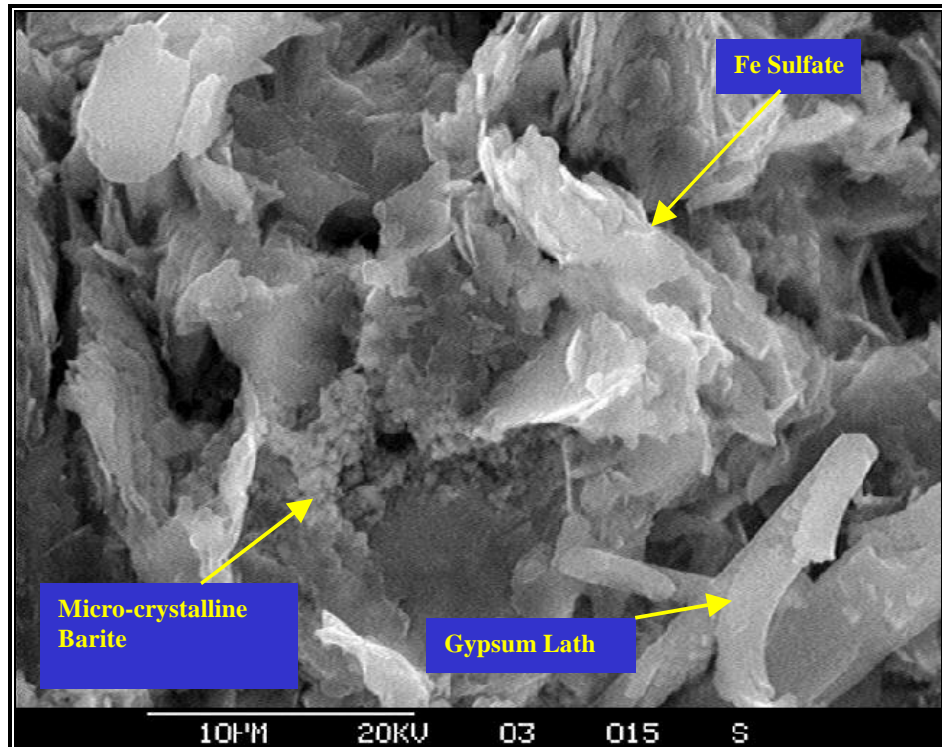

Figure 5.17: Micro-crystalline barite in the presence of ferrous sulfate and gypsum Site 4 (11.38 m)

Mineral morphology of the very fine tailings fraction (< 10 µm) is characterised by Figures 5.18, 5.19 and 5.20. Figure 5.18 shows a typical SEM field view in which the electron dense minerals (white appearance) such as uraninite and primary hematite occur in a groundmass of sub-crystalline magnesium sulfate, gypsum and amorphous iron and manganese oxides.

Magnesium sulfates occur as pervasive sub-crystalline amorphous phases. They are highly deliquescent and given their ubiquity, have the potential to reduce the relative humidity of the tailings and therefore its rate of evaporation (Emerson et al. 1994). Geochemical processes that have the potential to inhibit the rate of dewatering and hence tailings consolidation and strength need to be assessed and accounted for in closure planning and, more importantly, in the design of the capping structure. This is particularly important for in-pit closure as the great vertical thickness of the tailings could result in large differential settlement that may, in turn, compromise the long term integrity of the engineered cover. Figure 5.19 is a magnified view showing uraninite superimposed on gypsum.